

*Published in the Proceedings of the  
CEOS SAR Calibration Workshop  
(ESA WPP-048)*

**I**

**ERS-1 SAR RADIOMETRIC CALIBRATION**

**H. LAUR <sup>1</sup>, P. MEADOWS <sup>2</sup>, J.I. SANCHEZ <sup>1</sup>, E. DWYER <sup>1</sup>**

<sup>1</sup> European Space Agency/ ESRIN, Frascati, Italy

<sup>2</sup> GEC-Marconi Research Centre, Chelmsford, United Kingdom

\*\*\*\*\*

**II**

**ERS-1 SAR PRODUCTS VALIDATION**

**J.I. SANCHEZ, H. LAUR**

European Space Agency/ ESRIN, Frascati, Italy







*Published in the Proceedings of the  
CEOS SAR Calibration Workshop  
(ESA WPP-048)*

**I**

**ERS-1 SAR RADIOMETRIC CALIBRATION**

**H. LAUR<sup>1</sup>, P. MEADOWS<sup>2</sup>, J.I. SANCHEZ<sup>1</sup>, E. DWYER<sup>1</sup>**

<sup>1</sup> European Space Agency/ ESRIN, Frascati, Italy

<sup>2</sup> GEC-Marconi Research Centre, Chelmsford, United Kingdom

\*\*\*\*\*

**II**

**ERS-1 SAR PRODUCTS VALIDATION**

**J.I. SANCHEZ, H. LAUR**

European Space Agency/ ESRIN, Frascati, Italy









# ERS-1 SAR RADIOMETRIC CALIBRATION

H. LAUR <sup>1</sup>, P. MEADOWS <sup>2</sup>, J.I. SANCHEZ <sup>1</sup>, E. DWYER <sup>1</sup>

<sup>1</sup> European Space Agency / ESRIN, Frascati, Italy

<sup>2</sup> GEC-Marconi Research Centre, Chelmsford, United-Kingdom

## 1. INTRODUCTION

The European Space Agency perceives ERS SAR as an end to end system combining high on-board performances with accurate on-ground performance measurements, precise data processing and suitable transmission of data related information to the user community. Such a synergy between ERS space and ground segments is well illustrated by the SAR radiometric calibration activities. The combination of internal calibration parameters availability with accurate on-ground measurements gives to the ERS-1 user community the first opportunity to work with precisely calibrated SAR products acquired over a long time period.

This paper describes the status of the ERS-1 SAR radiometric calibration with updated measurements on the radiometric stability. The calibration measurements are performed using the transponders deployed by ESA/ESTEC in Flevoland, The Netherlands (Ref. 1). The calibration measurements are the result of a joint effort between the ESA Processing and Archiving Facilities (PAF) and the ERS Central Facility at ESA/ESRIN.

## 2. INTERNAL CALIBRATION PARAMETERS

Two types of internal calibration parameters are measured in the ERS-1 SAR Active Microwave Instrument (AMI). At the start and end of each SAR imaging sequence, a set of four calibration pulse measurements and eight noise measurements are made. During the imaging sequence, copies of the transmitted pulses (replicas) are generated and appended to the raw data. One complete replica pulse is transmitted with every 24 raw data range line records (Ref. 2).

These two stage internal calibration parameters are required to ensure that the ERS-1 SAR image products are internally calibrated, especially as the ERS-1 AMI does not have an automatic gain control system. The system gain can drift due to temperature changes and ageing. The gain changes are monitored via the replica pulse powers as they are passed through the SAR system. The calibration pulse measures the majority of the gain drift with the replica pulse being used to monitor the gain drift during the imaging sequence when the more representative pulse is not available. The thermal noise is measured when pulses are not being transmitted at the start and end of each imaging sequence.



## 2.1 Replica Pulses

Within the ESA SAR processors, a single replica pulse associated with the image product being processed is extracted and used for gain normalisation and range compression.

Two problems were identified with replica pulses. The first was that the replica pulse was being extracted from the raw data incorrectly such that the start of the replica was mis-identified by one or two range line records. The second problem was associated with the fact that the replica pulse itself is corrupt in that one or more of the 704 samples that make up the replica can have spurious values. This leads to a spike and/or null for one or more of the replica samples. The analysis of two raw data sets acquired during a corruption period shown that one in sixty replica pulses and one in every one hundred pulse were corrupt (Ref. 3).

The effect of these two problems on the resultant imagery was different at the UK-PAF and at the D-PAF (Ref. 4). For UK-PAF processed imagery, the only problem identified were streaks up to 10 km in length in range which emanated from bright point targets (Ref. 5). At the D-PAF, the images processed were severely corrupted. Quality checking has now been incorporated at the UK-PAF since April 1993 and at the D-PAF since May 1993 to identify the two problems and if found select another suitable replica pulse to be used for image generation.

### *Effect of the replica pulses corruption on the radiometric calibration :*

The use of a replica pulse within a processor assumes that the replica pulse power is directly proportional to the transmitted pulse power. Thus, if this were the case, any transmitter pulse power variations would be compensated for in the resultant SAR image. Figure 1 shows that the above assumption is invalid (i.e. there is no direct relationship between the replica pulse and calibration pulse power). Identical results are found by (Ref. 6). The consequence of this is that any replica pulse power variations introduced by a SAR processor need to be removed.

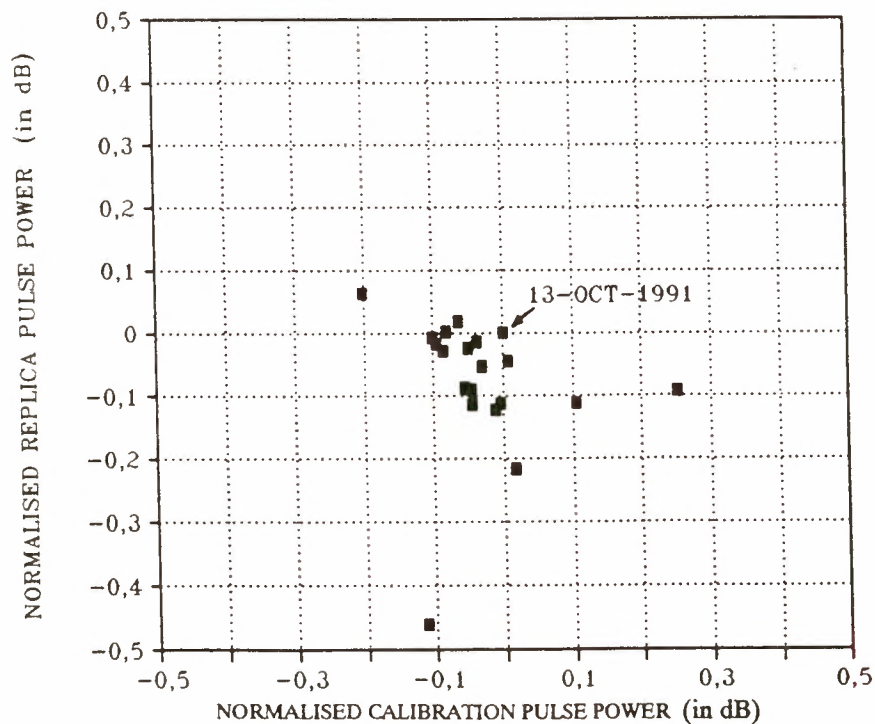


**Figure 1** *The relationship between replica and calibration pulse powers for Flevoland and Zeeland acquisitions during the commissioning and first ice phases. The values are normalised to the reference date (13 October 1991). The calibration pulse power is derived from the calibration pulses of the beginning of the acquisition sequences.*



Examination of the replica pulse power variations since the beginning of the ERS-1 mission in July 1991 (Figure 2) show that usually the replica pulse power is stable to within  $\pm 0.1$  dB but can, for short periods, be within a band of  $\pm 1.0$  dB. Identical results have been reported by (Refs. 7, 8).

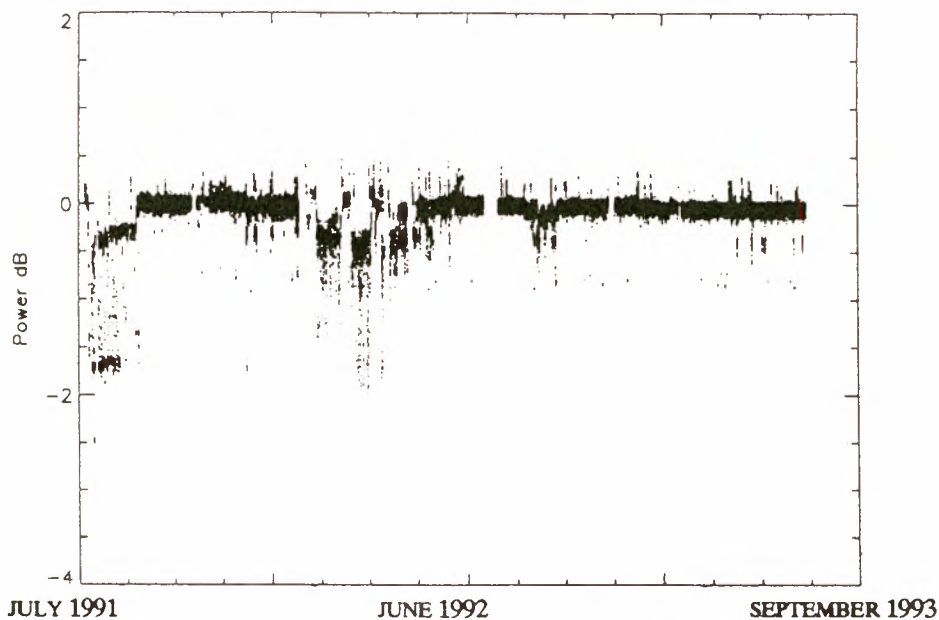


**Figure 2** *Replica pulse power variations since beginning of ERS-1 mission. The replica pulse power is normalised to the reference date (13 October 1991).*

From Figure 2, it can be seen that two main periods of high replica pulse power variations occurred since beginning of the ERS-1 mission :

- . during the early commissioning phase (from July to early October 1991)
- . during the early multi-disciplinary phase (from May to July 1992)

Periods when the replica power variations were higher than 0.4 dB correspond to 7.8 % of the acquisitions since beginning of the mission and 6.0 % of the acquisitions apart from the commissioning phase. 2.4 % of the acquisitions (mainly in August and September 1991) exhibit replica power variations higher than 1 dB. Figure 3 shows that in 1993 the variations of the replica pulse power are fairly small, i.e. within  $\pm 0.1$  dB.

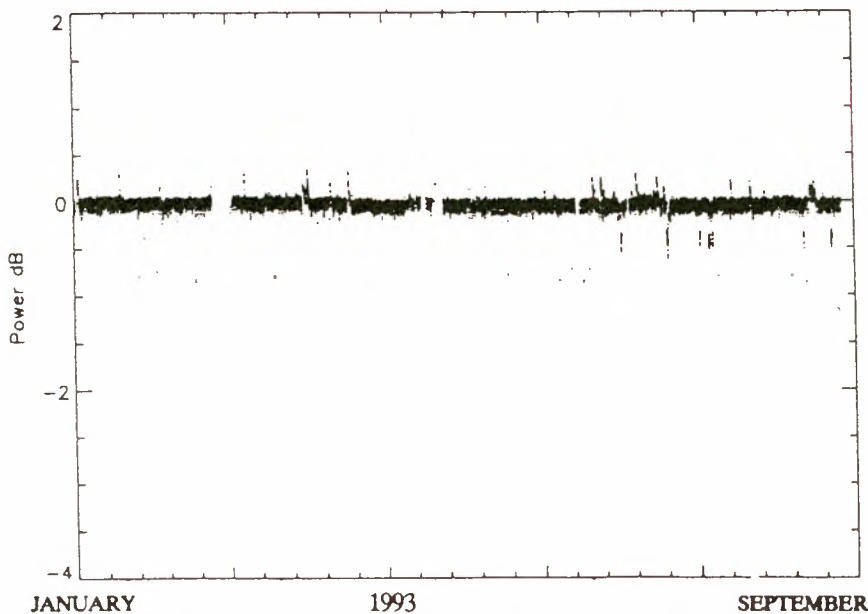


**Figure 3** *Replica pulse power variations during year 1993 (from January to September).*



Figure 4 shows that during the early commissioning phase, in September 1991, the replica pulse power variations were high. In fact during this period the descending passes (morning acquisitions over Europe) had a replica pulse power about 1.6 dB lower than the replica pulse power of the ascending passes (close to the mean reference value).

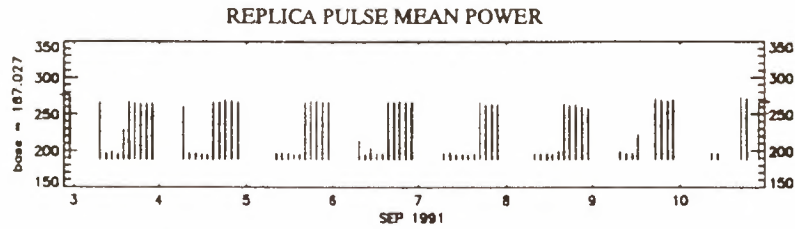


Figure 4 Replica pulse power variations from 3 to 10 September 1991.

During the Commissioning Phase, the imaging of the DRA Calibration Site at Romney-Marsh, Kent (Ref. 9) occurred during the descending passes. A comparison of point target powers and replica pulse powers (Figure 5) clearly shows a close link, i.e.: as the replica pulse power decreased, the point target powers increased by a similar amount (Ref. 10).

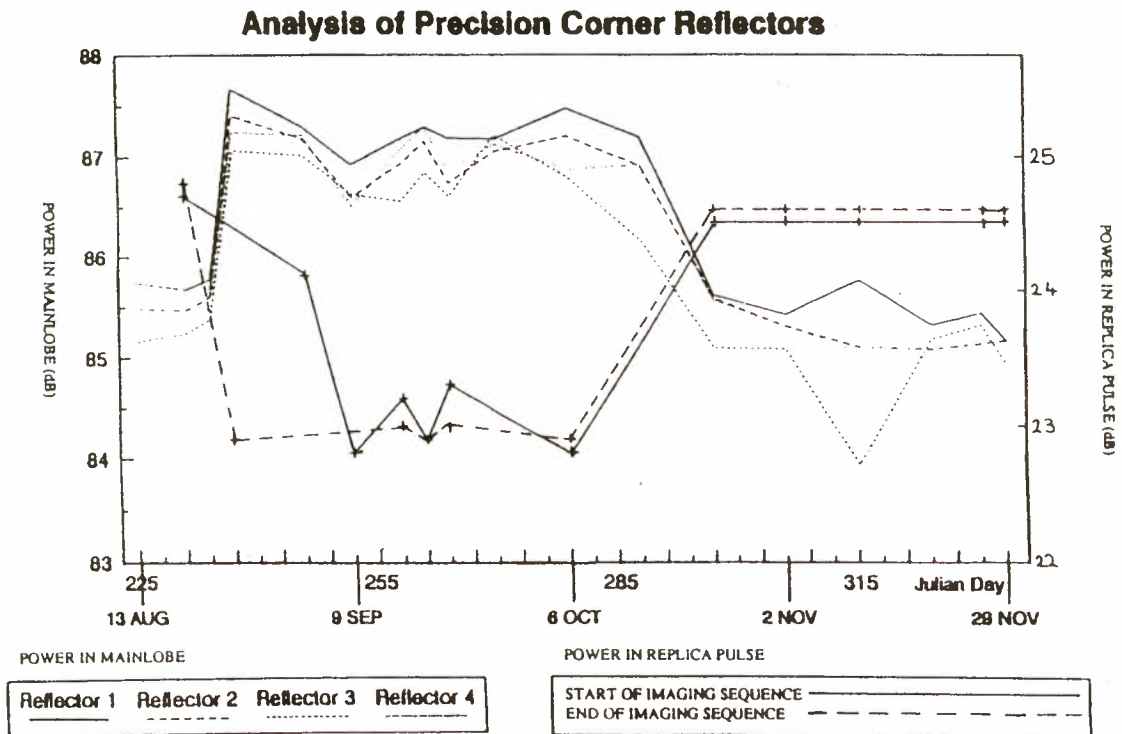


Figure 5 Variation in calibration point target power and replica pulse power during the commissioning phase (from analysis of DRA precision corner reflectors responses).

The imaging of the ESA calibration site in Flevoland (NL) occurred during the ascending passes when the replica pulse power was close to the reference value. The corrections to apply to the measured radar cross sections of the ESA transponders was lower than 0.5 dB during the commissioning phase.





Table 1 gives the values of the radiometric stability and the radiometric accuracy measured with the ESA transponder 2 before and after the correction of the replica pulse power variations.

Transponder 2 (38 measurements over 2 years)	before correction of replica pulse power variations	after correction of replica pulse power variations
<b>radiometric stability</b>	0.43 dB	0.38 dB
<b>radiometric accuracy</b>	0.38 dB	0.32 dB
<b>max. variation of the measured RCS</b>	± 0.92 dB	± 0.75 dB

**Table 1** Radiometric calibration measurements before and after correction of replica pulse power variations.

The **radiometric stability** is defined as the standard deviation of the (time serie) measurements of the radar cross section of a calibration target (using the same calibration constant) (Ref. 11).

The **radiometric accuracy** is defined as the (time serie) average of the absolute difference between the nominal radar cross section and the measured radar cross section (using the same calibration constant) of a calibration target (Ref. 11).

Similar results are found for transponders 1 and 3.

Users of ERS-1 SAR imagery need to correct their imagery to obtain correctly calibrated results. This is done by comparison of the replica pulse power used to generate the image in question with that used to generate the reference image of Flevoland from which the calibration constant was derived [13 October 1991] (Ref. 12). The replica pulse power used for image generation is given in the CEOS header of each image product. Similarly, users comparing two images need to take into account any difference in replica pulse powers.

The expression used for this correction is:

$$\frac{\text{image replica power}}{\text{reference replica power}}$$

As a consequence, the full expression to apply in order to determine the backscattering coefficient  $\sigma^0$  of an area located at incidence angle  $\alpha$  is (for an ESA SAR PRI product) :

$$\sigma^0 = \frac{\langle I \rangle}{K} \cdot \frac{\sin \alpha}{\sin \alpha_{\text{ref}}} \cdot \frac{\text{image replica power}}{\text{reference replica power}}$$

where  $\langle I \rangle$  is the mean pixel intensity,  $K$  the calibration constant and  $\alpha_{\text{ref}}$  the mid range incidence angle equal to 23 degrees.

The reference replica power is 205229 (value on 13 October 1991 at 21:40 UTC).



## 2.2 Calibration Pulses

Calibration pulse measurements are performed only at the start and the end of an imaging sequence. This creates practical difficulties. When the start or the end of the imaging sequence is outside the area of reception of an acquisition ground station. In such a case, the calibration pulses are not recorded. The calibration pulse power is the mean power of the 4 calibration pulses at the start and the end of the imaging sequence.

Since the beginning of the ERS-1 mission, the calibration pulse power appears stable: 87 % of the calibration pulse power measurements are within the range  $\pm 0.2$  dB. Figure 6 shows the variations of the calibration pulse power during the year 1993 (from January to September). The calibration pulse correction is by consequence fairly small.

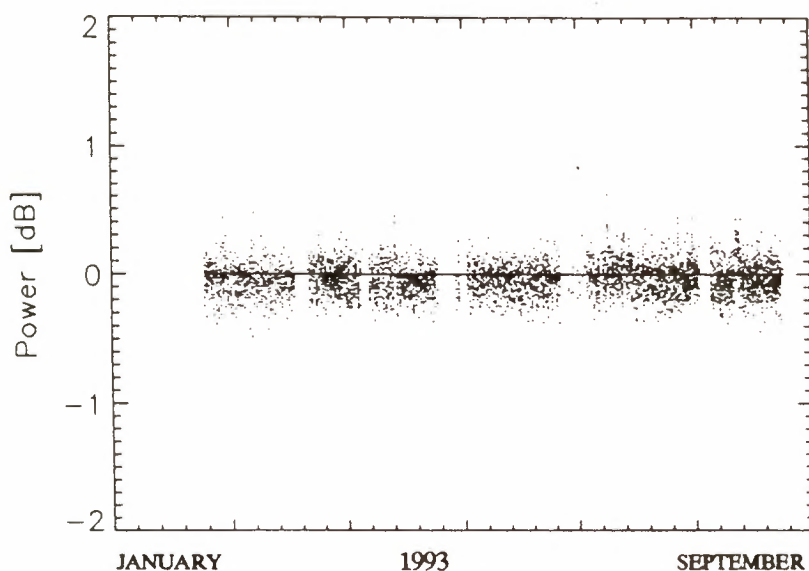


**Figure 6** Calibration pulse power variations during year 1993. The values are normalised to the reference date (13 October 1993).

When applied on ESA transponder responses, the calibration pulse correction does not improve the measurements results (see Table 2).

The correction has been applied on the original measurements and on the measurements previously corrected for the replica pulse power variations. The method of correction is similar to the one used for the replica pulse power correction with a reference value (calibration pulse power on 13 October 1991 at 21:40 UTC).

Transponder 2 (20 measurements during commissioning phase and ice phase)	original measurements	after correction of calibration pulse power variations	after correction of replica pulse power variations	after correction of replica & calibration pulse power variations
<b>radiometric stability</b>	0.36 dB	0.39 dB	0.33 dB	0.35 dB
<b>radiometric accuracy</b>	0.30 dB	0.33 dB	0.27 dB	0.29 dB

**Table 2** Radiometric calibration measurements before and after correction of calibration pulse power variations. The effect of the replica pulse power correction is shown for comparison.

No corrections are made for the calibration pulse power variations within the ESA ground segment SAR processors. Because the calibration pulse power information is difficult to access for users and because the correction of its variations do not improve the calibration measurements, it is not proposed to apply such a correction in the derivation of  $\sigma^0$  in ESA SAR products.



### 3. RAW DATA QUALITY PARAMETERS

#### 3.1 Raw Data Quality

SAR raw data obeys a certain statistical distribution (zero mean, Gaussian amplitude and uniform phase). Statistical checks on the data can establish whether the data has been corrupted during on-board processes such as in-phase (I) and quadrature (Q) channel separation and analogue to digital conversion (ADC).

A selection of parameters which can be derived from a block of raw data include (once the raw data for both channels have been suitably unpacked from 5 bit values to 8 bit values):

##### 1. I and Q Channel Means

This is the arithmetic mean of the data in the I and Q channels. The expected mean value in each channel is zero. Any bias on either channel can be easily corrected by subtracting the appropriate value from the I or Q channel values. This is indeed carried out for all ESA ground segment SAR processors. The I & Q channel means are stable parameters. Table 3 shows the stability of both channel means and a slight negative bias (corrected in the ESA processors).

Channel mean	Jan. 1992 to Sept. 1993 (18415 products)	May 1993 (837 products)	July 1993 (962 products)
I channel mean (mean $\pm$ s.d.)	- 0.158 $\pm$ 0.030	- 0.152 $\pm$ 0.028	- 0.159 $\pm$ 0.032
Q channel mean (mean $\pm$ s.d.)	- 0.137 $\pm$ 0.030	- 0.119 $\pm$ 0.029	- 0.107 $\pm$ 0.031

Table 3 I & Q channel mean from SAR products of different time periods.

##### 2. I and Q Channel Standard Deviations

This is the standard deviation of the data in the I and Q channels. For ERS-1 SAR image mode (On-Ground Range Compressed) the I and Q channels are quantised within the Analogue to Digital Convertor (ADC) to 5 bits each. This allows the quantised data to take integer values in the range -16 to 15 and with each channel having a Gaussian distribution. Thus, the distribution should have a maximum at 0 and should ideally fall to zero at -16 and 15. In addition, the ratio of the I and Q Standard Deviations (gain imbalance) should be one. Any gain imbalance can be corrected by multiplying the Q channel values by the gain imbalance. This is also carried out for all ESA ground segment SAR processors.

##### 3. I and Q Channel Top and Bottom Saturation

The saturation parameters are defined as the percentage of the samples occupying the highest or lowest quantisation levels for the I and Q channels.

The ERS-1 ADC can be easily simulated using routines to generate a Gaussian distribution with a zero mean and a specified input standard deviation together with quantisation to 5 bits for each of the channels. Figure 7 (from Ref. 6) shows histograms for the simulated I and Q channels for a selection of *input* standard deviations. When the *input* standard deviation has a value greater than approximately 5, tails in the distribution appear at the highest and lowest channel bins. This indicates that saturation has occurred in the top and bottom bins of the ADC. For each of the histograms, a Gaussian distribution has been derived and is superimposed on the histograms. The fitted Gaussian distribution is the one which was measured using



ERS-1 raw data (i.e. the ADC output parameters). Note that as the input standard deviation increases, the fitted Gaussian fails to fit the histogram.

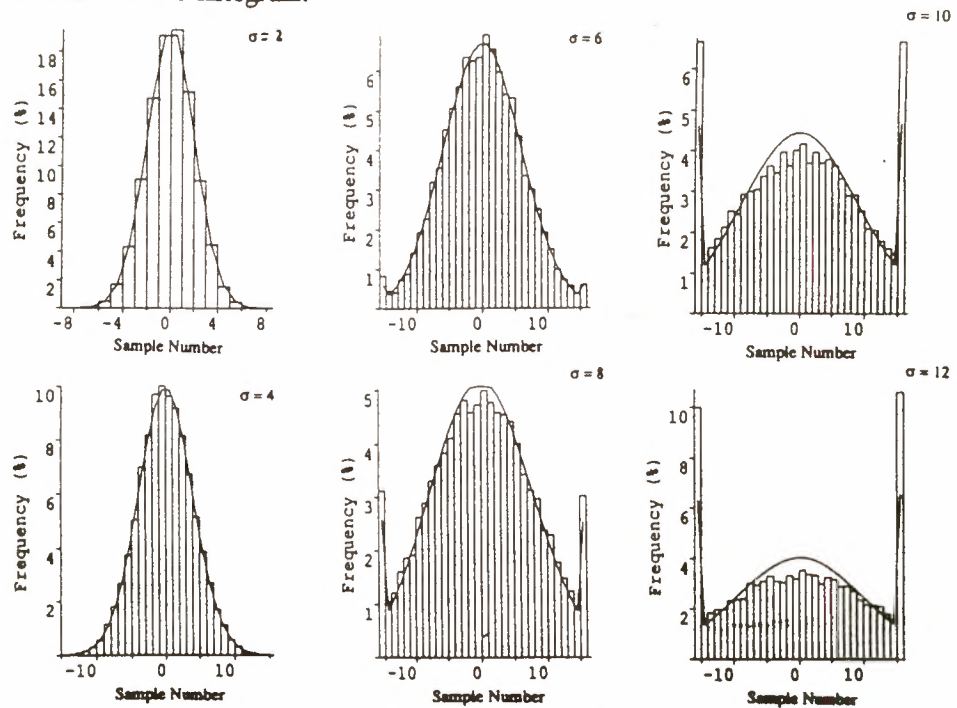


Figure 7 Simulated I & Q channels after quantisation by the ADC for various input standard deviations.

The zero mean used for the simulations is applicable for ERS-1 raw data as any non-zero bias is removed prior to processing as is any gain imbalance. The validity of using a Gaussian distribution can be deduced by comparing the simulated relationship between measured I & Q Top & Bottom Saturation and I & Q Standard Deviation values with actual ERS-1 raw data parameters. This has been carried out using a selection of raw data blocks from imaging sequences of Flevoland and Zeeland as Figure 8 (from Ref. 7) shows. The solid line in this figure is based on the simulations. A good agreement exists between the actual raw data and the simulations.

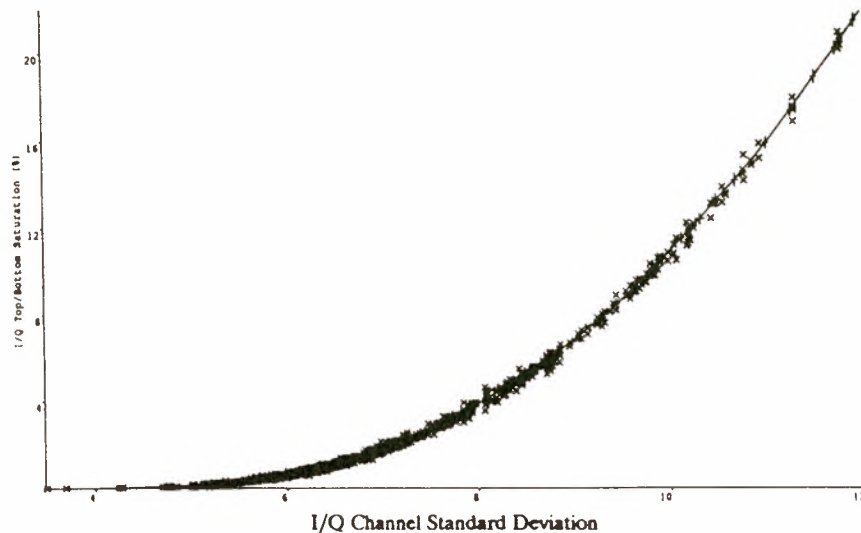


Figure 8 The relationship between I&Q channel standard deviation and I&Q top & bottom saturation for all the raw data blocks of the Flevoland and Zeeland image sequences. The solid line is derived from simulations using a zero mean Gaussian to represent the I&Q raw data channels.





The effect of saturation within the ADC leads not only to a difference in input and output standard deviations but more importantly to a difference in input and output powers. An ideal ADC should preserve the power of the raw data.

Figure 9 shows the difference between the simulated input and output ADC power as a function of *output* ADC standard deviation. This shows that for *output* standard deviations between 2 and 6, the power change introduced by the ERS-1 ADC is small (<0.1 dB). The power gain for small output standard deviations (<2) is a consequence of quantisation noise. For higher standard deviations, there is a significant power loss. This raw data power loss will be reflected in a correspondingly similar image power loss. Thus the high power losses have severe implications for distributed target radar cross-section measurements as well as for ERS-1 SAR radiometric stability determinations and ERS-1 SAR calibration.

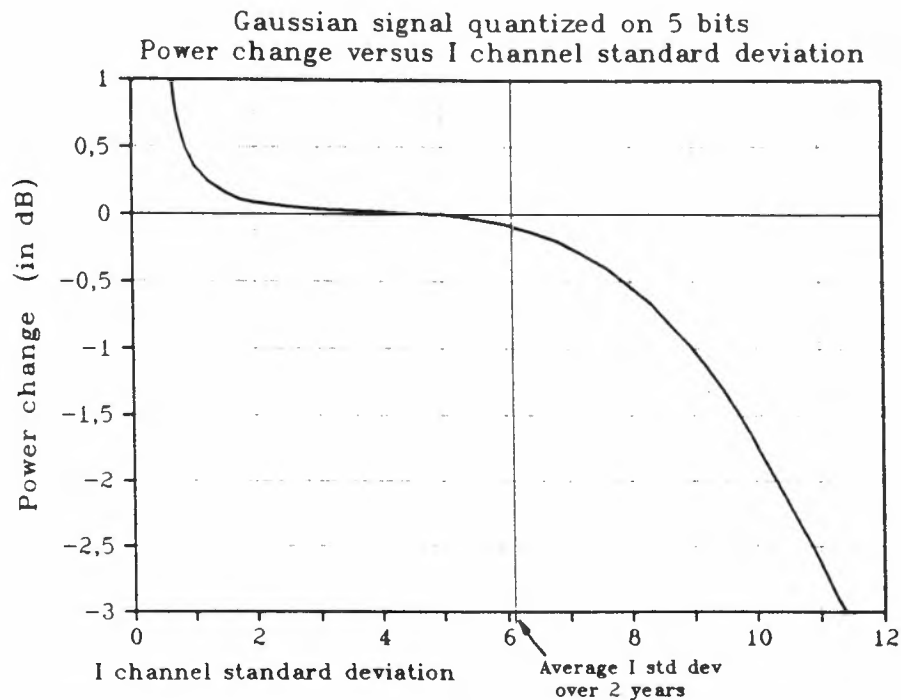


Figure 9 The ADC power change versus output I&Q channel standard deviation.

## 3.2 Effects of ADC saturation

### 3.2.1 Dependence of ADC power loss on surface types

Examination of ERS-1 SAR raw data for the period January 1992 to September 1993 indicate an average I channel standard deviation of 6.15 (corresponding to a power loss of 0.1 dB) together with a range of from approximately 2 to 12. These findings indicate that a significant proportion ( 22 % ) of the ERS-1 SAR raw data suffers from an ADC power loss higher than 0.5 dB.

Table 4 and Figure 10 give the monthly averages of the I channel standard deviation and the output image mean for a large quantity of SAR products. These SAR products correspond to acquisitions within the ESA ground stations of Kiruna (SW), Fucino (I) and Maspalomas (E), i.e. over Europe, North and West Africa, Greenland and North Atlantic.



Month	Number of SAR products analysed	Average I standard dev.	Output image mean
January 1992	1206	6.40	1779
February 1992	1151	6.25	1745
March 1992	1245	6.51	1787
April 1992	628	5.67	1627
May 1992	709	5.86	1542
June 1992	753	6.31	1816
July 1992	634	5.91	1510
August 1992	935	5.95	1589
September 1992	914	6.41	1781
October 1992	793	6.46	1748
November 1992	941	6.30	1872
December 1992	765	6.58	1809
January 1993	1147	5.91	1712
February 1993	977	6.07	1603
March 1993	1019	6.13	1606
April 1993	755	6.25	1580
May 1993	841	6.14	1562
June 1993	891	5.92	1613
July 1993	993	5.80	1485
August 1993	922	5.86	1470
September 1993	196	6.58	1627
Total	18415	6.15	1668

Table 4 Monthly average of I channel standard deviation and SAR image output mean.

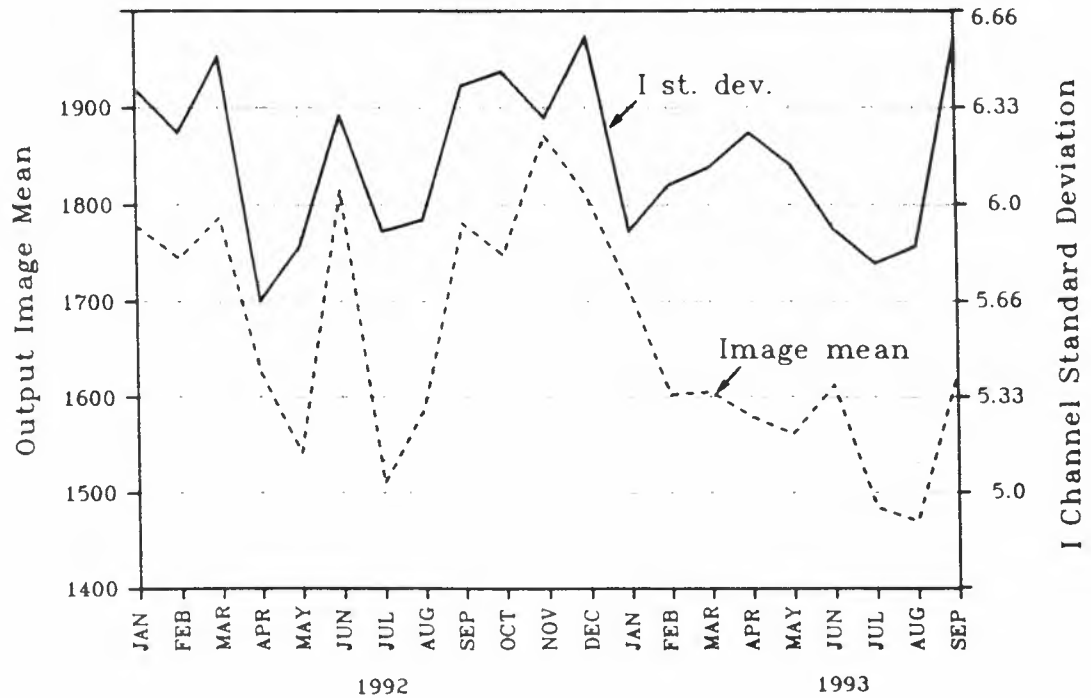


Figure 10 Monthly measurements of I channel standard deviation and image mean.



Table 5 gives a confirmation of the occurrence of ADC saturation mainly over sea areas.

Measurements from January 1992	Number of SAR products analysed	Average I standard dev.	Average ADC power loss
<i>Sea area</i> : Norwegian sea between lat. 60N & 70N between long. 12W & 3E	998	6.71	<b>0.18 dB</b>
<i>Sea area</i> : East Atlantic between lat. 40N & 60N between long. 20W & 10W	249	8.76	<b>0.87 dB</b>
<i>Land area</i> : Central Europe between lat. 47N & 52N between long. 10E & 30E	378	5.58	<b>0.03 dB</b>
<i>Land area</i> : France between lat. 44N & 50N between long. 0E & 7E	164	5.65	<b>0.04 dB</b>

**Table 5** *Average I channel standard deviation and ADC power loss over sea areas and land areas.*

The previous results give a global scale overview of ADC saturation. Examination of raw data products corresponding to an 100 km by 100 km ERS-1 image can be used to map the precise variation of I channel standard deviation and hence ADC power loss with location in the image and surface type. The raw data is examined by determining the standard deviation for a series of blocks. Each block has a range length equivalent to the replica pulse length (704 samples) and an azimuth length equivalent to the synthetic integration period (about 1300 samples). The blocks overlap each other by half a block size in both azimuth and range. For the raw data products examined below, the raw data has been sampled in range and azimuth by a factor of 10.

Two raw products (Kent, UK and Flevoland, NL) have been examined. Figure 12-a shows the I channel standard deviation in the form of a contour plot for Kent (orbit 865). The land mass of Kent is towards the top left of these plots while the English Channel occupies the remainder. Note that the highest standard deviations occur at near range and over the ocean. The average I channel standard deviation for each of these scenes is 7.44, while the range of values is 4.41 to 9.81. Clearly for this scene there is a significant variation in the I standard deviation. This variation is reflected in the power loss as Figure 12-b shows. A power loss of up to 1.5 dB occurs at near range which is coincident with the ocean. Over the land, the power loss is much less, except for coastal regions.

Figure 13-a shows the I channel standard deviation of a Flevoland scene for the calibration reference date (13 October 1991). The Flevoland polder is at the bottom centre of these plots while the IJsselmeer is at the centre. Note that the highest standard deviations occur once again at near range and over the ocean. Figure 13-b shows the power loss over the scene. The power loss is as high as 0.65 dB over Flevoland. The measured power loss in a raw data block centred on transponder 2 is 0.39 dB.



As expected, the image mean is correlated with the I channel standard deviation. Figure 10 shows an increase of the output image mean during winter. This is an effect of the storms over the North Atlantic ocean during winter. This suggests that the ADC saturation occurs mainly over large areas having an high backscattering level (e.g. water surface during storms). Figure 11 confirms this suggestion.

Figure 11 is a map of I channel standard deviation over Western and Central Europe. The black triangle indicates a scene with I channel standard deviation (for the whole 100 x 100 km scene) higher than 7, i.e. an ADC power loss higher than 0.25 dB. The diamond indicates a scene with I channel standard deviation lower than 7. The map shows that ADC saturation occurs mainly over the sea.



**Figure 11** Map of I channel standard deviation over Europe. The ADC saturation (black triangles) occurs mainly over the sea.





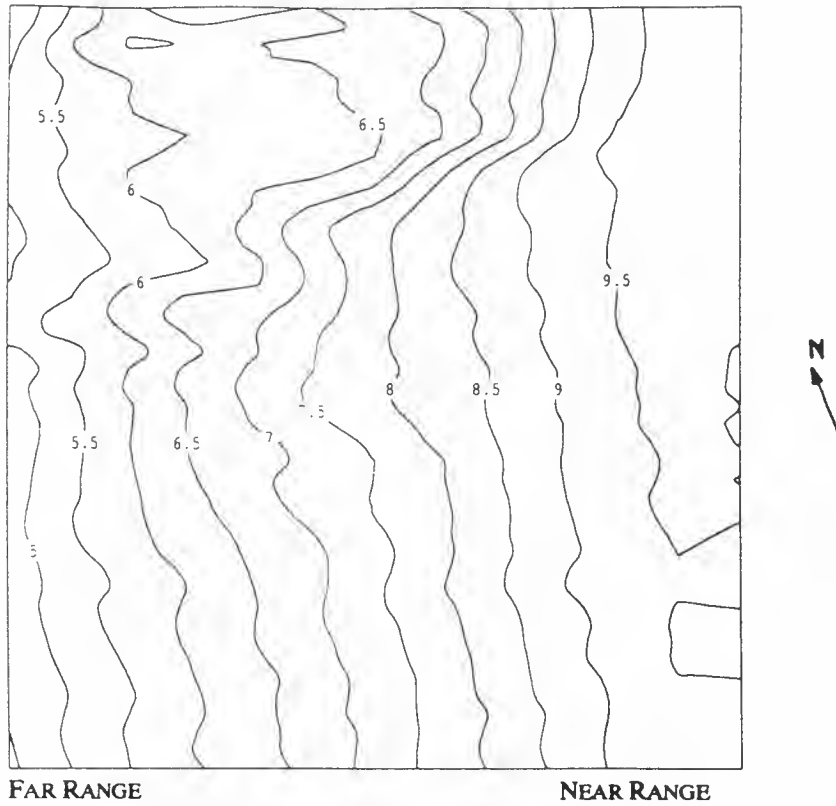


**Figure 12-a** *I channel standard deviation of a raw data scene over Kent (UK). The scene covers an area of about 105 x 105 km and has been acquired on 15 September 1991. The Kent coast is in the top left of the scene. The English Channel occupies the rest of the scene. Note the high values of I channel standard deviation over the sea, particularly at near range.*

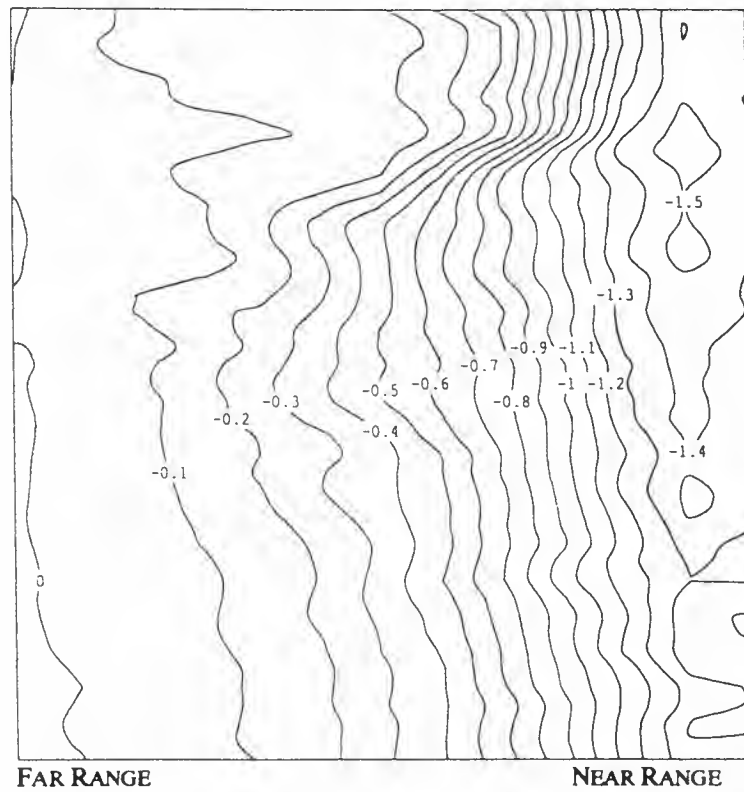


**Figure 12-b** *ADC power loss over Kent (15 September 1991). Note that the ADC power loss is as high as 1.5 dB at near range. Over land the ADC power loss is less than 0.2 dB.*



I Channel Standard Deviation

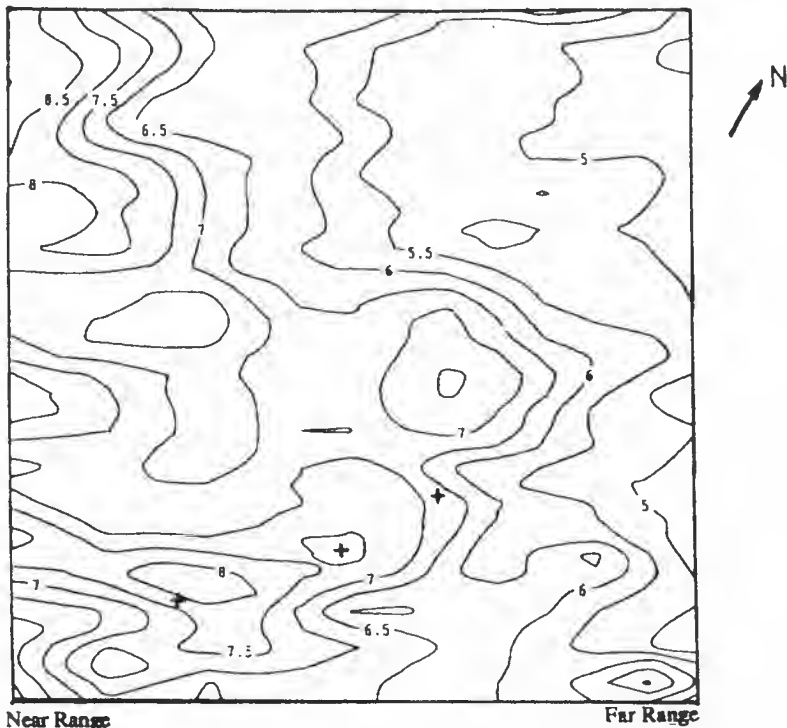


Figure 13-a

*I* channel standard deviation of a raw data scene over Flevoland (NL). The scene covers an area of about 105 x 105 km and has been acquired on 13 October 1991 (reference date for calibration constant derivation). The IJsselmeer is in the middle in the image and the Flevoland polder in the bottom centre. The transponders location is indicated by a cross (see Figure 14)

ADC Power Change

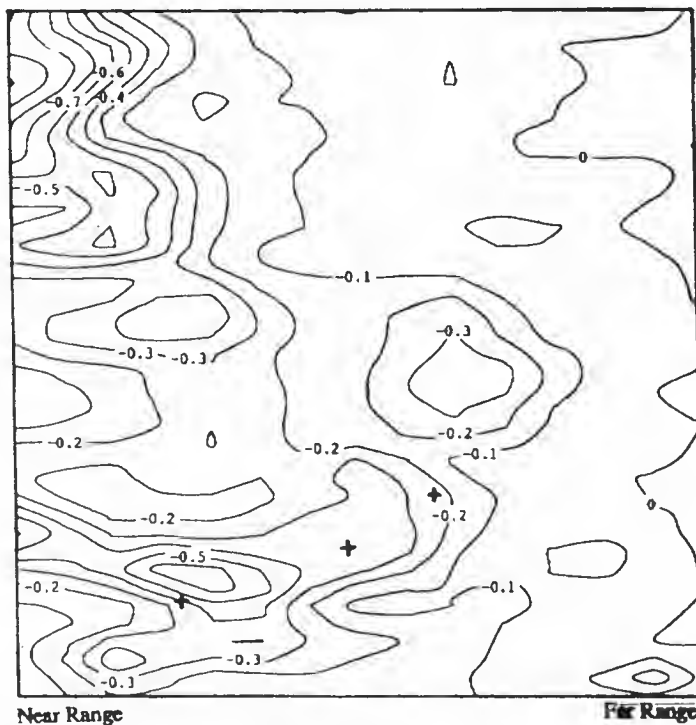


Figure 13-b

ADC power loss over Flevoland (13 October 1991). Note the ADC power loss values in Flevoland polder area ranging from 0.2 dB to 0.5 dB (see Figure 14).



### 3.2.2 Implications for the radiometric stability measurements

The previous results clearly indicate the need to correct for ADC non-linearities when measuring the radar cross sections of calibration target, especially when the target is located close to the sea (coastal area). In such a case the raw data would be required for the correction analysis. This means practical difficulties when a big number of scenes have to be analysed.

Another solution, provided by the SAR Verification Mode Processor (VMP) installed at ESA/ESRIN and at the D-PAF, is to generate a raw data power table for each processed product. Each entry in the table corresponds to the mean power of a block of raw data. The raw data block size is approximately the synthetic aperture length (1300 range lines) in the azimuth direction and the replica length (704 samples) in the range direction.

The average power of the raw data from each block is given by :

$$P_o = \frac{1}{NM} \sum_{k=1}^N \sum_{j=1}^M (I^2 + Q^2)$$

where N = number of range lines used  
M = number of samples used per line

From the raw data power table is derived an ADC nonlinearity correction table using the table and figures given in chapter 3.1.

The ESA transponders are then located in the table in order to apply the ADC nonlinearity correction to their measured radar cross section. The location of the transponders is done with the following method:

#### *Azimuth direction:*

The transponder is first located in the image (PRI product) by its pixel position in metres relative to the first pixel of the first image line. Then the time shift  $\Delta t$  between the first raw data line (defined by the acquisition time) and the first image line (defined by the zero Doppler azimuth time of the first azimuth pixel) is calculated and converted in position shift using the satellite ground velocity ( $V_g = 6640$  m/s) :

$$\text{Azimuth position(Raw data table)} = \text{Azimuth position(PRI product)} + (\Delta t \cdot V_g)$$

#### *Ground range direction:*

The transponder is located in the image (PRI product) by its pixel position in metres relative to the first pixel of the first image line. This value is converted in slant range position. Half of the replica length (352 samples) is then subtracted to take into account discarding of samples during range compression:

$$\text{Range position(Raw data table)} = \text{Slant range position(PRI product)} - 352 \text{ samples}$$

When the transponder is located close to the limit between two blocks in the ADC correction table, then an average is done between the two blocks.

Table 6 gives the ADC correction to be applied on the measured radar cross sections of the ESA transponders during the commissioning phase and first ice phase. During the commissioning phase the transponders were located in Flevoland. During the first ice phase, they were located in Zeeland (Figure 14).



	ADC correction to applied on measured R.C.S. (values in dB)		
	Transponder 1	Transponder 2	Transponder 3
<b>Commissioning Phase (Flevoland)</b>			
07-SEP-1991	0.28	0.06	0.05
19-SEP	0.17	0.17	0.00
25-SEP	0.30	0.26	n.d.
01-OCT	1.98	0.57	0.39
07-OCT	0.32	0.22	0.26
13-OCT	0.30	0.39	0.21
19-OCT	0.67	0.32	0.38
25-OCT	0.25	0.30	n.d.
31-OCT	0.24	0.09	0.04
06-NOV	0.75	0.88	0.57
12-NOV	1.05	1.34	1.00
18-NOV	0.62	1.11	0.81
24-NOV	0.52	0.76	0.54
30-NOV	0.35	0.73	0.33
06-DEC	0.57	0.48	0.49
<b>First Ice Phase (Zeeland)</b>			
11-JAN-1992	0.42	0.17	n.d.
17-JAN	n.d.	0.80	0.37
23-JAN	0.17	0.05	0.02
29-JAN	0.40	0.30	0.12
01-FEB	0.40	0.03	0.06
10-FEB	1.17	0.62	0.34
16-FEB	1.00	0.77	0.56
22-FEB	1.39	0.69	0.32
28-FEB	0.21	0.13	0.22
05-MAR	0.96	0.41	0.32
08-MAR	0.26	0.28	0.06
11-MAR	0.61	0.37	0.18
<b>Flevoland + Zeeland</b>			
Mean ± Standard deviation			
27 dates	0.59 ± 0.43	0.45 ± 0.33	0.32 ± 0.25
<b>Flevoland only</b>			
Mean ± Standard deviation			
15 dates	0.56 ± 0.45	0.51 ± 0.37	0.39 ± 0.29
Incidence angle	20.7 deg.	22.7 deg.	23.6 deg.
<b>Zeeland only</b>			
Mean ± Standard deviation			
12 dates	0.64 ± 0.40	0.39 ± 0.26	0.23 ± 0.16
Incidence angle	20.4 deg.	23.1 deg.	26.0 deg.

n.d. = no data

**Table 6**

*ADC non-linearity corrections to apply on the measured radar cross sections of the ESA transponders in Flevoland and Zeeland.*





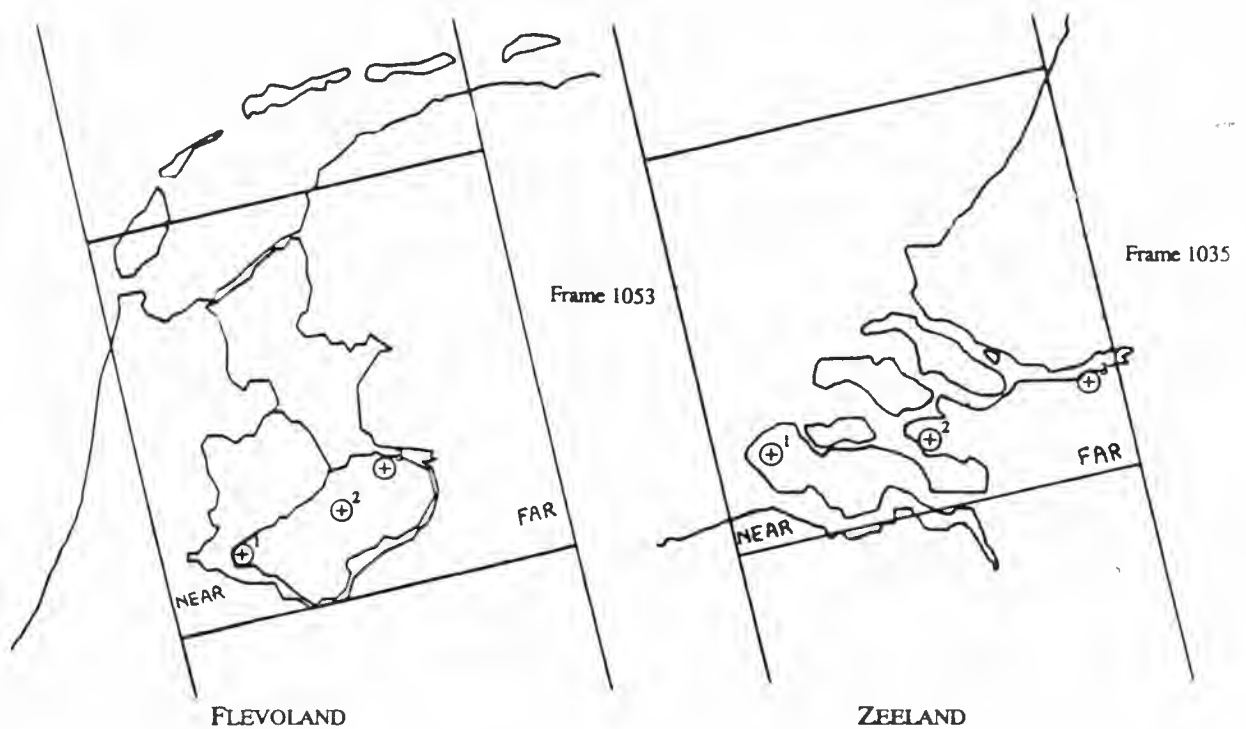


**Figure 14** Localisation of the ESA transponders in Flevoland (Commissioning Phase and Multi-Disciplinary Phase) and Zeeland (Ice Phases).

The mean ADC non-linearity correction for the transponders depends on two effects (for both calibration sites):

- **the transponder location in range:** the mean ADC correction decreases along range from 0.59 dB at near range (mean incidence angle of about 20.5 degrees for transponder 1) to 0.32 dB at far range (mean incidence angle of about 24.8 degrees for transponder 3). This an effect of the elevation antenna pattern.
- **the vicinity of high backscattering large distributed targets** (e.g. rough water surface areas): this is reflected by the standard deviation of the ADC correction. Transponder 1 is located close from the IJsselmeer during the commissioning phase and close to the North Sea during the first ice phase. The areas of open water can produce a wide range of backscattering levels according to the state of the water surface and by consequence a large range of ADC correction to apply. As an example, a scene over Flevoland acquired on 14 March 1993 exhibits very low backscattering for the IJsselmeer. Figure 15-a & b are plots of I channel standard deviation of the scene and ADC power change. Note that the I channel standard deviation can be as low as 1.04, which gives actually a positive ADC power change (i.e. a power gain) of up to 0.3 dB.



### I Channel Standard Deviation

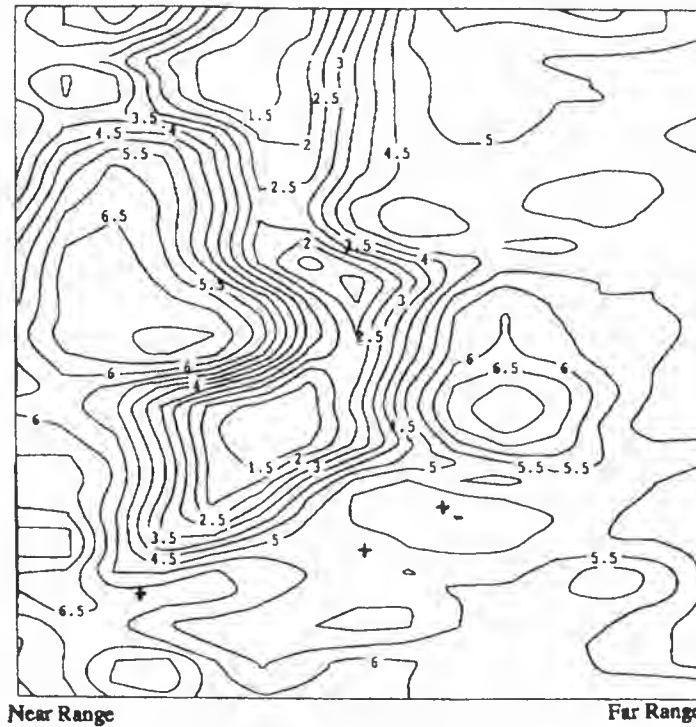


**Figure 15-a** *I channel standard deviation of a raw data scene over Flevoland (NL). The scene covers an area of about 105 x 105 km and has been acquired on 14 March 1993. Very low values of I channel standard deviation (down to 1.04) can be seen in the IJsselmeer. The lake has a very low backscattering level.*

### ADC Power Change

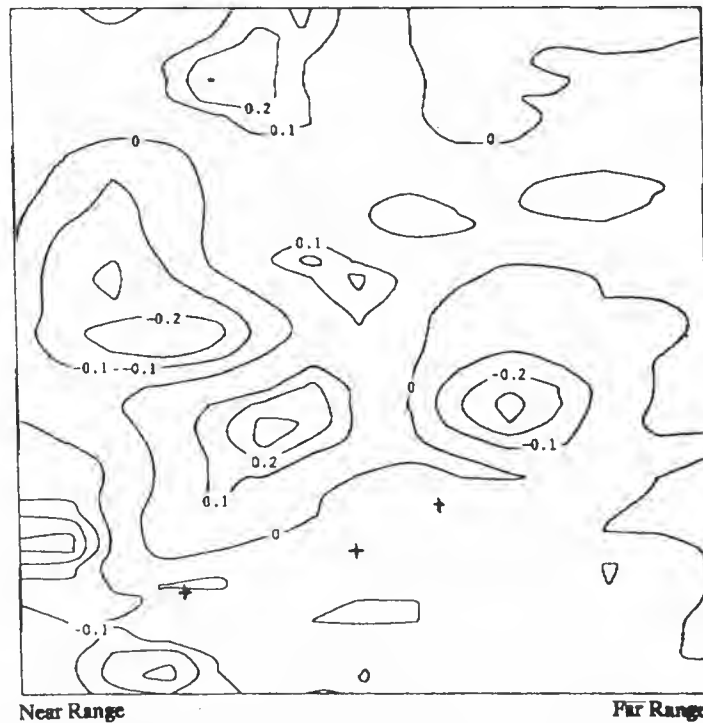


**Figure 15-b** *ADC power loss over Flevoland (14 March 1993). Note that there is no ADC correction to apply on the transponder responses.*



Table 7 gives the values of the radiometric stability and the radiometric accuracy measured with the transponder 2 before and after the ADC correction. The values before the ADC correction are values corrected for the replica pulse power variations.

Transponder 2 (38 measurements over 2 years)	before correction of ADC power loss estimate	after correction of ADC power loss estimate
<b>radiometric stability</b>	0.38 dB	<b>0.18 dB</b>
<b>radiometric accuracy</b>	0.32 dB	<b>0.16 dB</b>
<b>max. variation of the measured RCS</b>	± 0.75 dB	<b>± 0.42 dB</b>

**Table 7** *Radiometric calibration parameters with correction of ADC non-linearities.*

Similar results are found for transponders 1 and 3. Detailed results are shown in Table 8.

From the results in table 7, it appears that *the ADC non-linearities correction gives a substantial improvement in the precision of the radar cross sections measurements*. The derived radiometric parameters like the radiometric stability and the radiometric accuracy are *reduced by half*.

Due to the high precision of the previously derived parameters, further radiometric corrections (which are usually neglected in SAR radiometric calibration) can be applied in the derivation of the ERS-1 calibration measurements. Potentials corrections are :

- correction of distributed target ambiguity
- correction of atmospheric propagation loss



All values are in Decibels	Measured RCS			Measured RCS with Replica Pulse Variations Correction			Measured RCS with ADC Non-linearities Correction			Measured RCS with updated calibration constant (+ 0.39 dB)		
	Tr. 1	Tr. 2	Tr. 3	Tr. 1	Tr. 2	Tr. 3	Tr. 1	Tr. 2	Tr. 3	Tr. 1	Tr. 2	Tr. 3
<b>Commissioning Phase - Flevoland</b>												
07-SEP-1991	0.60	0.68	0.56	0.14	0.22	0.10	0.42	0.28	0.15	0.03	-0.11	-0.24
19-SEP-1991	0.55	0.61	0.65	0.28	0.34	0.38	0.45	0.51	0.38	0.06	0.12	-0.01
25-SEP-1991	0.34	0.34	n.d.	0.07	0.07	n.d.	0.37	0.33	n.d.	-0.02	-0.06	n.d.
01-OCT-1991	-0.88	0.19	0.29	-1.10	-0.03	0.07	0.88	0.54	0.46	0.49	0.15	0.07
07-OCT-1991	0.42	0.57	0.68	0.17	0.32	0.43	0.49	0.54	0.69	0.10	0.15	0.30
13-OCT-1991	-0.03	<b>0.00</b>	-0.09	-0.03	<b>0.00</b>	-0.09	0.27	<b>0.39</b>	0.12	-0.12	<b>0.00</b>	-0.27
19-OCT-1991	-0.28	0.10	-0.56	-0.28	0.10	-0.56	0.39	0.42	-0.18	0.00	0.03	-0.57
25-OCT-1991	0.04	-0.03	n.d.	0.03	-0.04	n.d.	0.28	0.26	n.d.	-0.11	-0.13	n.d.
31-OCT-1991	0.18	0.34	0.21	0.16	0.32	0.19	0.40	0.41	0.23	0.01	0.02	-0.16
06-NOV-1991	-0.60	-0.19	-0.29	-0.54	-0.13	-0.23	0.21	0.75	0.34	-0.18	0.36	-0.05
12-NOV-1991	-0.59	-0.81	-0.86	-0.52	-0.74	-0.79	0.53	0.60	0.21	0.14	0.21	-0.18
18-NOV-1991	0.03	-0.61	-0.74	0.05	-0.59	-0.72	0.67	0.52	0.09	0.28	0.13	-0.30
24-NOV-1991	-0.28	-0.38	-0.61	-0.28	-0.38	-0.61	0.24	0.38	-0.07	-0.15	-0.01	-0.46
30-NOV-1991	-0.16	-0.08	-0.45	-0.18	-0.10	-0.47	0.17	0.63	-0.14	-0.22	0.24	-0.53
06-DEC-1991	-0.34	-0.01	-0.32	-0.34	-0.01	-0.32	0.23	0.47	0.17	-0.16	0.08	-0.22
<b>First Ice Phase - Zeeland</b>												
11-JAN-1992	0.23	0.33	n.d.	0.20	0.30	n.d.	0.62	0.47	n.d.	0.23	0.08	n.d.
17-JAN-1992	n.d.	-0.14	-0.07	n.d.	-0.15	-0.08	n.d.	0.65	0.29	n.d.	0.26	-0.10
23-JAN-1992	0.56	0.71	0.30	0.51	0.66	0.25	0.68	0.71	0.27	0.29	0.32	-0.12
29-JAN-1992	0.06	0.47	0.19	-0.05	0.36	0.08	0.35	0.66	0.20	-0.04	0.27	-0.19
01-FEB-1992	-0.27	0.54	n.d.	-0.32	0.49	n.d.	0.08	0.52	n.d.	-0.31	0.15	n.d.
10-FEB-1992	-0.52	-0.13	-0.15	-0.63	-0.24	-0.26	0.54	0.38	0.08	0.15	-0.01	-0.31
16-FEB-1992	-0.70	-0.15	-0.39	-0.81	-0.26	-0.50	0.19	0.51	0.06	-0.20	0.12	-0.33
22-FEB-1992	-0.37	-0.33	0.05	-0.48	-0.44	-0.06	0.91	0.25	0.26	0.52	-0.14	-0.13
28-FEB-1992	0.39	0.46	-0.16	0.30	0.37	-0.25	0.51	0.50	-0.03	0.12	0.11	-0.42
05-MAR-1992	-0.30	-0.24	n.d.	-0.39	-0.33	n.d.	0.57	0.08	n.d.	0.18	-0.31	n.d.
08-MAR-1992	0.13	0.41	0.18	0.04	0.32	0.09	0.30	0.60	0.15	-0.09	0.21	-0.24
11-MAR-1992	-0.15	0.11	0.32	-0.27	-0.01	0.20	0.34	0.36	0.38	-0.05	-0.03	-0.01
<b>Multi-Disciplinary Phase - Flevoland</b>												
03-MAY-1992	0.71	1.03	0.77	0.34	0.66	0.40	0.49	0.68	0.59	0.10	0.29	0.20
07-JUN-1992	0.55	0.81	0.55	0.15	0.41	0.15	0.42	0.57	0.36	0.03	0.18	-0.03
12-JUL-1992	n.d.	0.54	0.42	n.d.	0.44	0.32	n.d.	0.53	0.49	n.d.	0.14	0.10
20-SEP-1992	n.d.	0.57	0.53	n.d.	0.50	0.46	n.d.	0.57	0.54	n.d.	0.18	0.15
25-OCT-1992	n.d.	n.d.	-0.44	n.d.	n.d.	-0.52	n.d.	n.d.	0.09	n.d.	n.d.	-0.30
29-NOV-1992	n.d.	-0.60	-0.48	n.d.	-0.83	-0.71	n.d.	-0.09	0.07	n.d.	-0.48	-0.32
03-JAN-1993	n.d.	n.d.	0.56	n.d.	n.d.	0.45	n.d.	n.d.	0.47	n.d.	n.d.	0.08
14-MAR-1993	0.51	0.65	0.64	0.42	0.56	0.55	0.45	0.56	0.60	0.06	0.17	0.21
18-APR-1993	-1.03	-0.28	-0.91	-1.02	-0.27	-0.90	-0.24	0.41	-0.08	-0.63	0.02	-0.47
23-MAY-1993	n.d.	0.39	0.47	n.d.	0.29	0.37	n.d.	0.31	0.38	n.d.	-0.08	-0.01
27-JUN-1993	0.20	0.59	0.53	0.11	0.50	0.44	0.32	0.52	0.47	-0.07	0.13	0.08
01-AUG-1993	0.22	0.18	0.12	0.11	0.07	0.01	0.34	0.33	0.19	-0.05	-0.06	-0.18
Mean	-0.02	0.17	0.05	-0.13	0.07	-0.06	0.40	0.45	0.25	0.01	0.06	-0.14
Standard Dev.	0.45	<b>0.43</b>	0.48	0.40	<b>0.38</b>	0.41	0.22	<b>0.18</b>	0.22	0.22	0.18	0.22
Max. Range	1.74	1.84	1.68	1.61	1.49	1.46	1.15	0.84	0.87	1.15	0.84	0.87

n.d. = no data

**Table 8** R.C.S. measurements of the transponders over 2 years (only ascending passes). The values are expressed in decibels. They are referenced to the measured radar cross section of transponder 2 on 13th October 1991. The same calibration constant  $K$  is used to derive these measurements, except for the last columns set where the updated calibration constant  $K_u$  ( $K_u = K + 0.39$  dB) is used. The standard deviation of the measurements is by definition the radiometric stability.





### 3.2.3 Implications for the derivation of the calibration constant

The calibration constants for ESA ERS-1 products are derived from transponder 2 radar cross section on 13 October 1991 (Ref. 12). The estimation of the ADC non-linearities correction (computed from the raw data block power analysis) to apply on transponder 2 radar cross section for this date is 0.39 dB (see Table 6). A confirmation of the estimate is given by the mean ADC correction of 0.45 dB. An updated calibration constant is obtained when applying the ADC correction:

$$K(\text{updated}) = K + 0.39 \text{ dB}$$

The updated calibration constant  $K$  is *consistent* with previous  $K$  estimate error bounds given at the end of the commissioning phase. The updated  $K$  error bounds  $\pm 0.42$  dB are indeed within the previous estimation of  $\pm 0.75$  dB (Figure 16).

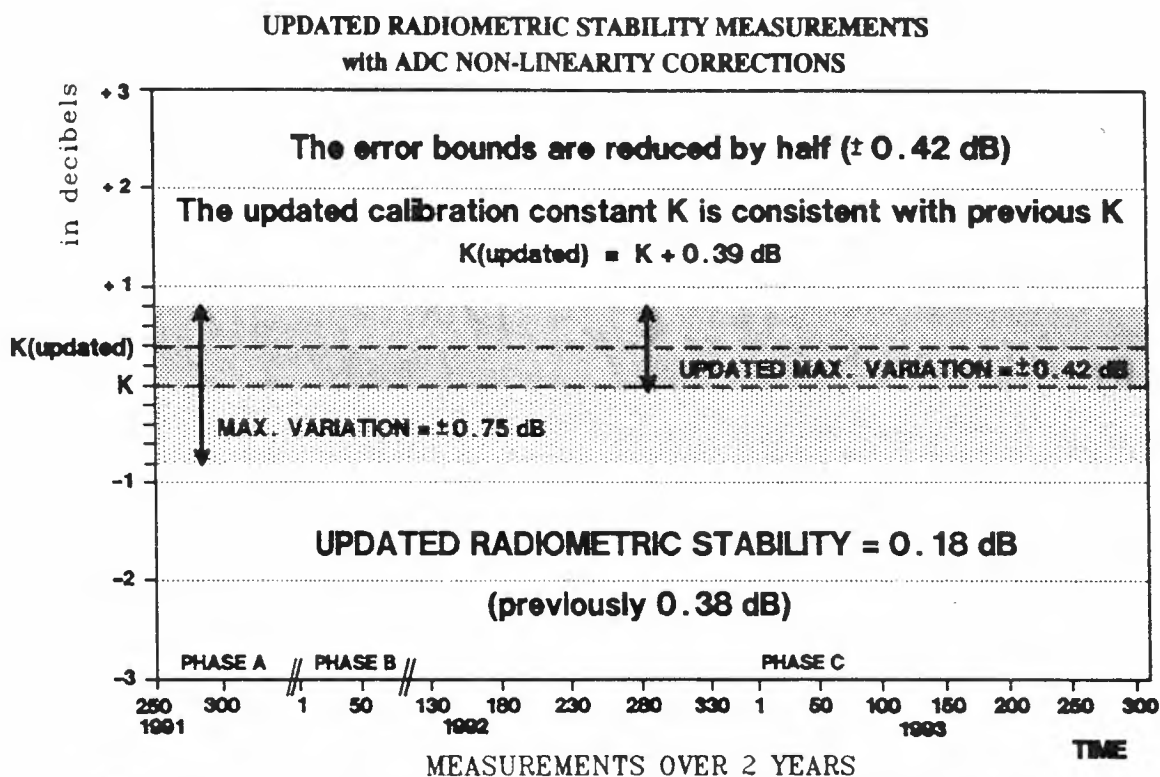


Figure 16 Updated radiometric stability measurements with ADC non-linearity correction.

### 3.2.4 Implications for the derivation of the in-flight antenna pattern

The in-flight ERS-1 SAR antenna elevation pattern has been estimated using detected images over the Brazilian rain forest. The derivation of the antenna pattern was done using the mean range profile of 10 images of uniform rain forest with the assumption that  $\gamma = \sigma^0 / \cos \alpha$  is a constant value for the rain forest (for the ERS-1 SAR incidence angles  $\alpha$ ). The derived mean polynomial of range profiles was set to zero at the boresight angle (look angle  $\theta = 20.35$  degrees). Noise compensation was applied. The estimated in-flight antenna pattern was then compensated in ESA PRI product (Ref. 12).

In order to check the effect of ADC non-linearities over the rain forest, a raw data image was analysed. Figure 17 gives the contour plots of the I channel standard deviation of the scene. The derived ADC power loss in the scene versus the look angle  $\theta$  is given in Figure 18.



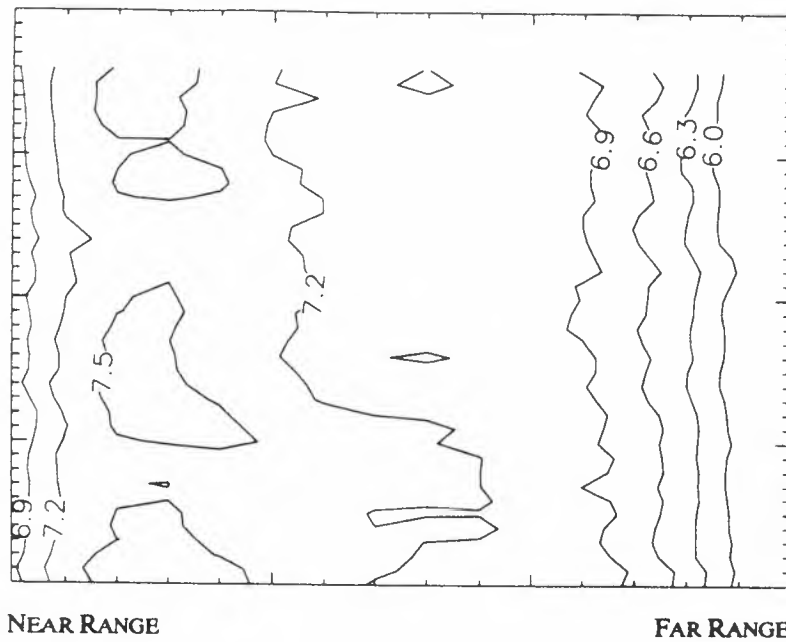


**Figure 17** *I* channel standard deviation of a raw data scene over the Brazilian rain forest. Note the high values of *I* channel standard deviation at near range.

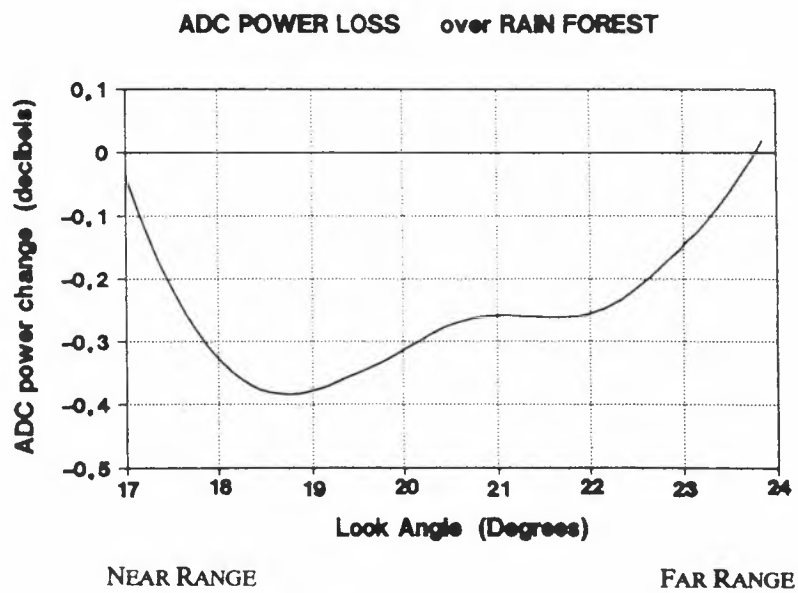


**Figure 18** *ADC* power loss in the preceding scene (Figure 17).



The estimated ADC power loss correction is then applied on the previously derived in-flight antenna pattern. The new estimation of the antenna pattern has then to be set to zero at boresight angle in order to be comparable with the previous one. The result is given in Figure 19.

Figure 20 shows the difference between the new and previous antenna pattern estimation. Note that the difference is lower than 0.1 dB in the scene except at extreme far range (up to 0.3 dB).

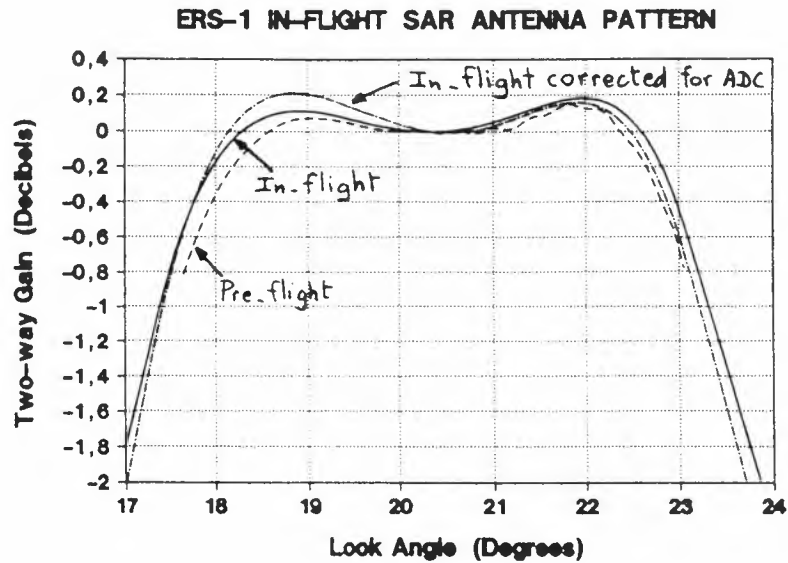


Figure 19 ERS-1 in-flight antenna pattern estimations.

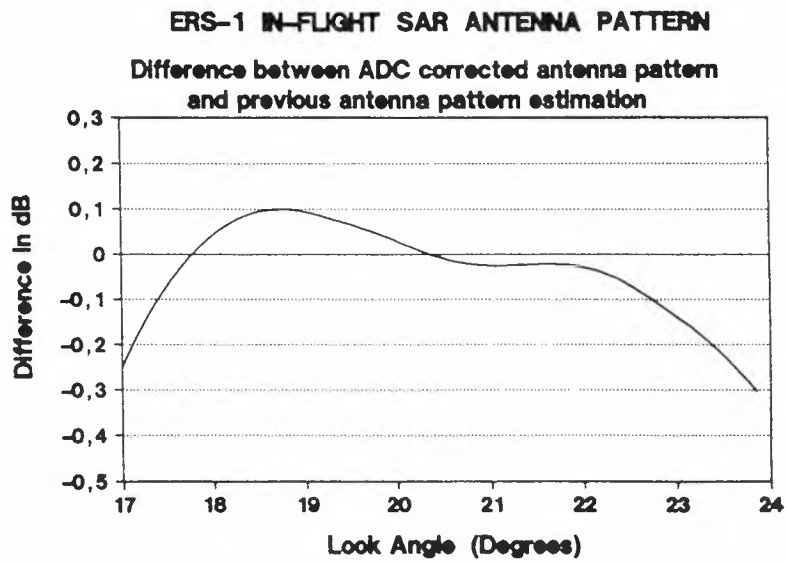


Figure 20 Difference between ADC corrected antenna pattern and previous antenna pattern estimations.



#### 4. CONCLUSIONS

This study confirms the high radiometric stability of the ERS-1 SAR since beginning of the mission. When including the Analogic to Digital Converter (ADC) non-linearity corrections, we obtain a reduction by half of the radiometric calibration parameters such as the radiometric accuracy or the radiometric stability. The values of the calibration constants previously given within maximum bounds of about  $\pm 0.8$  dB are now given within maximum bounds of about  $\pm 0.4$  dB. The radiometric stability measured over two years is about 0.2 dB, well within the specifications.

The study has identified the ADC non-linearity as the main source of errors in the measurements of radar cross sections or backscattering coefficients. The ADC non-linearity occurs over large distributed targets having high backscattering level such as rough sea surfaces.

ERS-1 SAR calibration requirements have been carefully established following expert recommendations. One of these recommendations formulated ten years ago (Ref. 13) was the following : "*Calibration of ERS-1 to a level of  $\pm 1$  dB would be a major achievement*".

#### ACKNOWLEDGMENTS

The authors wish to thank their ESA colleagues (including M. Doherty and E. Attema) for useful discussions and the ESA Processing and Archiving Facilities of Germany and United Kingdom for their contribution.

#### REFERENCES

1. H.D. Jackson & A. Woode, 'Development of the ERS-1 Active Radar Calibration Unit', *IEEE Trans. on Microwave Theory and Techniques*, Vol. 40, No. 6, pp. 1063-1069, June 1992.
2. D.C. Lancashire, 'ERS-1 AMI Calibration and Characterisation Plan', *Marconi Space Systems Report*, ER-PL-MSS-AM-0008, Issue 13, March 1987.
3. P.J. Meadows, 'ERS-1.SAR.RAW Replica Pulse Analysis', *GEC-Marconi Research Centre Report*, PF-TN-MRC-0002, Issue 2.0, October 1992.
4. J. Sanchez & H. Laur, 'ERS-1 SAR Products Validation', *to appear in same proceedings*, September 1993.
5. P.J. Meadows, 'The Effect of using Corrupt Replica Pulses on UK-PAF Processed ERS-1.SAR.PRI Imagery', *GEC-Marconi Research Centre Report*, PF-TN-MRC-0005, Issue 1.0, December 1992.
6. P.J. Meadows, 'ERS-1.SAR.PRI Status Report', *GEC-Marconi Research Centre Report*, PF-TN-MRC-0006, Issue 1.0, January 1993.
7. B. Schättler, W. Noack, H. Wilhelms, 'Die Verarbeitung von SAR-Daten des ERS-1 bei der D-PAF', *Proceedings of the 8th Radar Symposium*, Neupirg, pp. 186-191, September 1993.





8. P.A. Wright, 'ERS-1 SAR CATA of the Raw Data Quality Parameters and the Internal Calibration Parameters for September 1991 to December 1992', *GEC-Marconi Research Centre Report*, PF-TN-MRC-0010, Issue 1.0, June 1993.
9. P.J. Bird, D.R.D. Kenward, G.E. Keyte, 'An Experiment for the Radiometric Calibration of the ERS-1 SAR', *Proceedings of the First ERS-1 Symposium*, Cannes, ESA SP-359, pp. 195-200, November 1992.
10. P.J. Meadows & C.M. Stapleton, 'Replica Pulse Power and Absolute Calibration Scaling Factor Variations', *GEC-Marconi Research Centre Report*, PF-TN-MRC-0001, Issue 1.0, September 1992.
11. GEC-Marconi Research Centre, 'SAR Data Quality Assessment and Rectification', *ESA contract report No. 6635/86/HGE-I*, March 1988.
12. H. Laur, 'ERS-1 SAR Calibration: Derivation of Backscattering Coefficient  $\sigma^0$  in ERS-1.SAR.PRI Products', *ESA/ESRIN Technical Note*, Issue 1, Rev. 0, October 1992.
13. 'Radar Calibration', *Proceedings of EARSEL Workshop*, Alpbach, Austria, December 1982.







## ESA ERS-1 SAR CALIBRATION CONSTANTS

*The calibration constants are valid for any acquisitions  
between 5 September 1991 and 30 September 1993.*

*The calibration constants are given within bounds of  $\pm 0.75$  dB.*

<b>PRI product</b>			
<b>processed after 1st September 1992</b>			
<b>ESRIN/EECF</b>	<b>D-PAF</b>	<b>UK-PAF</b>	<b>I-PAF</b>
<b>K = 666 110</b> <b>= 58.24 dB</b>	<b>K = 666 110</b> <b>= 58.24 dB</b>	<b>K = 890 107.2</b> <b>= 59.49 dB</b>	<b>K = 791 334</b> <b>= 58.98 dB</b>

<b>PRI product</b>		
<b>processed before 1st September 1992</b>		
<b>ESRIN/EECF</b>	<b>D-PAF</b>	<b>UK-PAF</b>
<b>K = 678 813</b> <b>= 58.32 dB</b>	<b>K = 678 813</b> <b>= 58.32 dB</b>	<b>K = 890 107.2</b> <b>= 59.49 dB</b>

<b>SLC product</b>		
<b>ESRIN/EECF</b>	<b>D-PAF</b>	<b>UK-PAF</b>
<b>K = 65 026</b> <b>= 48.13 dB</b>	<b>K = 65 026</b> <b>= 48.13 dB</b>	<b>K = 47 021.4</b> <b>= 46.72 dB</b>
	<i>processed before 15 Nov. 1992 :</i> <b>K = 186 618 = 52.27 dB</b>	

Following the results of a recently published study [*ERS-1 SAR Radiometric Calibration, H. Laur et al., to be published in the Proceedings of the CEOS SAR Calibration Workshop, ESA WPP-048*], users who need a more accurate estimation of the calibration constant can use the following formula :

$$K_{\text{updated}} = K + 0.39 \text{ dB}$$

with bounds of  $\pm 0.42$  dB. Please note that the updated value of K is still within the previously given bounds of  $\pm 0.75$  dB.









## II

### ERS-1 SAR PRODUCTS VALIDATION

Sánchez J.I., Laur H.

ESA/ESRIN  
Frascati  
Italy

#### ABSTRACT

Validation and quality monitoring of the ERS-1 SAR products is a vital task in order to ensure the success of the ERS 1 mission. This article explains the criteria used during the validation of ERS-1 SAR products (image mode) as well as the quality procedures implemented to control systematically the production in the ground stations and in the PAFs (Processing and Archiving Facility), once the products have been validated.

Some key quality results obtained after the two first years of mission are also presented.

Keywords: ERS-1, SAR, Validation, Quality, PAF, Ground Station.

#### 1. INTRODUCTION

Since July 1991, ERS-1 has been providing the international community with a huge amount of data. To allow the exploitation of the data by the international scientific community and also by commercial users, a major effort must be invested in monitoring the quality and the consistency of the SAR products processed within the decentralised ESA ERS-1 ground segment.

#### 2. SAR PRODUCT VALIDATION

##### 2.1 ESA SAR Product Validation

##### 2.1.1. ESA SAR Products

The ESA ERS-1 ground segment has been established using a decentralised set of processing facilities with central monitoring and control at ESA/ESRIN (EECF=ESRIN ERS Central Facility). The ERS-1 SAR products are generated at the ESA ground stations (Fucino, Kiruna and Maspalomas), at the PAFs (D-PAF at Oberpfaffenhofen, I-PAF at Matera and UK-PAF at Farnborough) and at ESA/ESRIN.

Four processors are involved in the generation of SAR products:

- **Fast Delivery Processor (FDP)** at the ground stations

Provided by MDA  
DEC VAX 6210  
2 ST 50 Array Processors

- **Verification Mode Processor (VMP)** at D-PAF and ESRIN

Provided by MDA  
DEC VAX 6210  
2 ST 50 Array Processors.



- **EMMA 2 Processor** at I-PAF

Provided by Telespazio/ELSAG  
DEC VAX 6005  
Special dedicated processor EMMA 2

- **EODC SAR processor** at UK-PAF

Provided by EDS SCICON  
Microvax + Amteck  
3 numeric array processors

In addition two geocoding systems, GEOS at D PAF and GEO at I PAF (under validation) are responsible for production of the geocoded products:

- **GEOS system** at D PAF

Provided by DLR/IPI/RSL/DIBAG  
SUN SparcStations (SUN4)

- **GEO system** at I PAF

Provided by Telespazio  
VAX 9000  
Vector processing option

The different products generated are:

- **RAW**: annotated raw data in 8 bit format
- **SLC**: single look, complex, slant range image in 16 bit format (quarter scene)
- **UI16, FDC (UI16 off-line copy), PRI**: three look, detected, ground range image in 16 bit format
- **GEC**: Geocoded Ellipsoid Corrected product, derived from PRI
- **GTC**: Geocoded Terrain Corrected product, derived from PRI

A complete product description can be found in the document **ESA ERS-1 Product specification (ESA SP-1149)**.

### **2.1.2 Strategy and status of validation.**

The main tool used at ESA/ESRIN to analyse, validate and calibrate the SAR products is the **SARCALQ** system (SAR CALibration & Quality analysis) developed by EDS Scicon.

Fast delivery image quality is systematically monitored. Periodic updates of the FDP software have been performed to continuously improve the FDP's performance. Since February 1993 FDP SAR 4.2 processor has been running in all the ground stations. As the processing performed by the FDP SAR processor is simpler than that done by the off-line processors (e.g., there is not antenna pattern correction), anomalies are also less frequent.

Before a PAF starts to produce images operationally, the product must be validated by ESA/ESRIN. The PAF forwards a validation report with some examples (digital product on exabyte or on CCT, and photographic hardcopies), to ESA/ESRIN. After analysis, the product is either validated or recommendations are made for improvement of the product quality.

ESA/ESRIN and the PAFs work together to bring the different products inside the specifications previously determined by ESA.

Different checks are carried out:

- **Image Visual Inspection**



- Point Target QA (FDC, SLC, PRI)
  - Spatial resolution (3 dB width in azimuth and range)
  - Peak to Side-Lobe Ratio
  - Integrated Side-Lobe ratio
  - Localisation Accuracy
  - Radar Cross Section (for PRI & SLC product)
- Distributed target QA (FDC, SLC, PRI)
  - Radiometric resolution
  - Backscattering coefficients (for PRI product)
  - Verification of the antenna pattern implementation

In addition the linearity of the processor has to be demonstrated (with point targets and distributed targets).

For geocoded products the residuals (distance between a point in the image and the real position in the map) are measured. It is also verified that the geocoding processing retains the radiometric characteristics of the scene.

Different reference scenes have been chosen to perform the measurements needed to establish the quality of the product. The main test site is the Flevoland area in The Netherlands. Three transponders have been deployed by ESA/ESTEC in this area to allow the calibration and the quality analysis of ERS-1 SAR products. The transponder produces in the image the Impulse Response Function of the system. This IRF is used to determine some of the radiometric characteristics of the SAR image as well as the localisation accuracy of the scenes.

Additional test sites are found in Zeeland (NL)(during the ice phases the ESA transponders are moved to this area), Kent (UK/DRA calibration test site), ...Low and high latitude scenes are also used to investigate problems which may be due to latitude (e.g. antenna pattern correction).The Frankfurt area is the test scene used to control the quality of geocoded products. This area presents a mean height value of about 250 m, and an irregular relief.

The current status of the validation is summarised in the next table. To date 20 products have been validated with 5 different processors.

#### On-Line SAR Image Product

Detected Data	UI16	Fucino (I), Maspalomas (S), Kiruna (SW)	through satellite link
---------------	------	---	------------------------

#### Off-Line SAR Image Product

Raw Data	RAW	D-PAF, EECF, I-PAF, UK-PAF	Telemetry Data + Annotations
Complex Data	SLC	D-PAF, EECF, I-PAF	Quarter Frame, Bandwidth=1400 Hz
	SLCF	UK-PAF	Full Frame, Bandwidth=1100 Hz
Detected Data	PRI	D-PAF, EECF, I-PAF, U-PAF	Pixel 12.5x12.5m, radiometrically corrected
	FDC	D-PAF, EECF	Pixel 16x20m, not radiometrically corrected
Ellipsoid Corrected	GEC	D-PAF, <i>I-PAF*</i>	From PRI product
Terrain Corrected	GTC01	D-PAF	If Digital Elevation Model available
	GTC02	D-PAF	If Digital Elevation Model available

**Figure 1:** Table showing the validation status of ESA ERS-1 SAR image products

\* The GEC product from I PAF is under validation



## 2.2. National & foreign stations SAR product validation

All around the world, different agencies are acquiring and processing ERS-1 SAR data. These agencies must demonstrate the quality of the ERS-1 SAR product that they generate. To control the products, the following information must be provided by the stations to ESA/ESRIN:

- Description of the SAR Processor
- Detailed SAR Products Specification
- Detailed Validation Procedures and Results
- Sample Products on CCT or Exabyte and on Slides (with annotations)

The stations validated to date are:

- Fairbanks (NASA/UAF,USA)
- Gatineau + Prince Albert (CCRS,Canada)
- Tromsø (TSS,Norway)
- Aussaguel (CNES,France)
- Hyderabad (NRSA,India)
- Alice Springs (ACRES,Australia)

## 3. QUALITY MONITORING

### 3.1. SAR performance monitoring

Systematically, the three ESA ground stations send to ESA/ESRIN the annotations of all the fast delivery images processed. These headers contain important information as to where and when the data were collected, the parameters used in the processing, quality flags showing the status of the communications link and statistical information about the raw data and the final image product. Other information about the noise measurements, calibration pulse and chirp replica is also sent. All this information is kept in a database at ESA/ESRIN to allow the monitoring and further investigation of trends or anomalies that may appear in the satellite's performance or in the image data acquired.

Daily, some UI16 samples are also sent from the stations, and backed up at ESA/ESRIN. These products are used to carry out further investigations after detection of anomalies. A report is produced monthly by ESA/ESRIN showing the results of the month's investigation. The next three figures (fig. 2,3 & 4) illustrate some of the controls performed at ESA/ESRIN to ensure the quality of the ERS-1 SAR products.

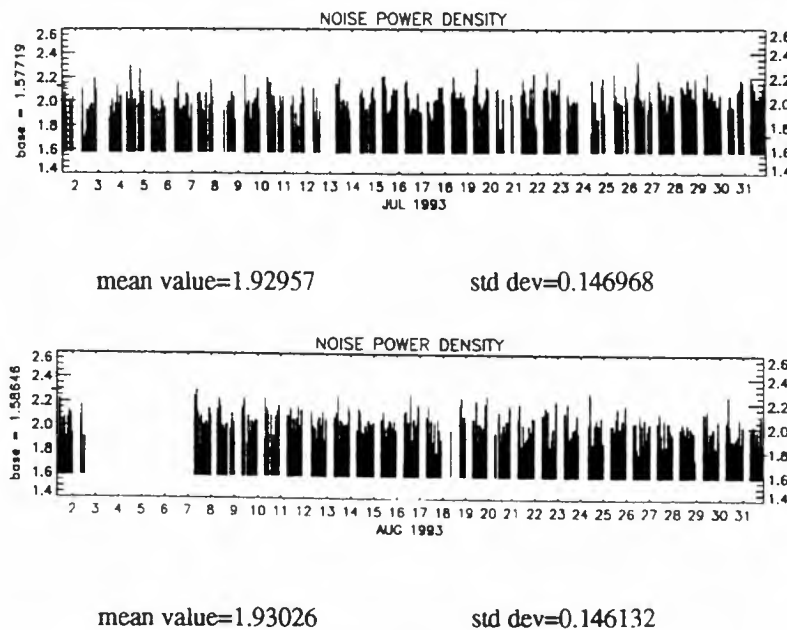


Figure 2: Comparison of noise power in the radar system (July and August 1993)





From fig.1 and fig.2 it is possible to compare the noise power density during July 1993 against the same parameter measured during August 1993.

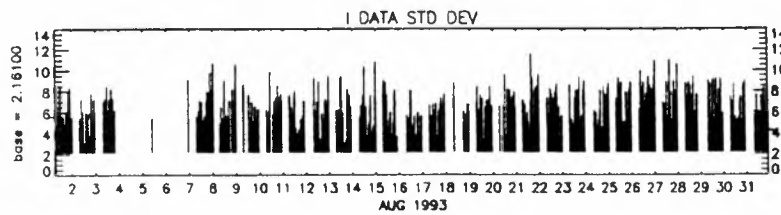


Figure 3: Raw data I channel std dev during August 1993

Figure 3 shows the *standard deviation* of the *raw data* in the *I channel* during August 1993. This information indicates if there is saturation in the raw data recorded by the satellite. This saturation has an important effect in every SAR Image product generated, independently of the processor used.

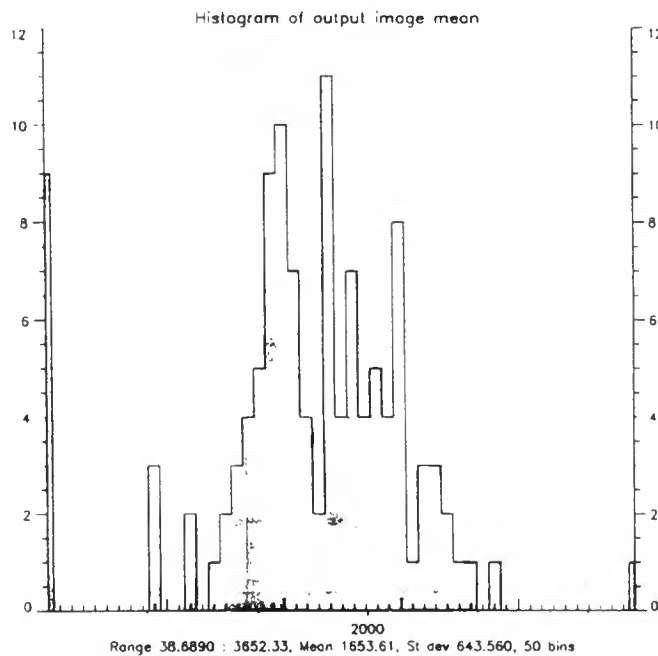


Figure 4: Mean output value histogram of the FD products processed at Fucino station during February 1993

Figure 4 shows a histogram of the *mean output value* of fast delivery images produced at Fucino station during February 1993. Because of a problem in the parameters used to process the data after the installation of a new FDP software version, Fucino station was producing low quality products for more than one week. These products had an output mean much lower than normal. After detection of the problem corrective actions were taken to resolve it.

### 3.2. SAR Image product quality results

The user community should have identical product quality independent of the ESA processor used to process the raw data. In other words, the ESA facility providing the SAR product should be transparent to the user. Unfortunately, different hardware and software means that it is very difficult to achieve exactly the same performance everywhere.

This table summarises the characteristics of the different products in the different PAFs.



<i>PRI</i>	<i>ESRIN/D-PAF</i>	<i>UK-PAF</i>	<i>I-PAF</i>	<i>ESA Spec.</i>
range resolution	24.88 m	24.5 m	29.62 m	< 30 m
azimuth resolution	21.5 m	20.00 m	24.04 m	< 30 m
islr	-9.44 dB	-14.20 dB	-9.75 dB	< -8 dB
range peak side lobe ratio	-20.73 dB	< -21 dB <sup>1</sup>	-22.83 dB	< -18 dB
azimuth peak side lobe ratio	-16.43 dB	< -21 dB <sup>1</sup>	-20.21 dB	< -18 dB

<i>SLC</i>	<i>ESRIN/D-PAF</i>	<i>UK-PAF<sup>2</sup></i>	<i>I-PAF</i>	<i>ESA Spec.</i>
range resolution	9.8 m	9.48 m	9.60 m	< 10 m
azimuth resolution	5.3 m	5.27 m	6.05 m	< 10 m
islr	-14 dB	-10.47 dB	-14.55 dB	< -8 dB
range peak side lobe ratio	-22.37 dB	-13.99 dB	-18.63 dB	< -18 dB
azimuth peak side lobe ratio	-28.4 dB	-24.45 dB	-29.59 dB	< -18 dB

**Figure 5: PRI and SLC quality parameters for the different PAFs**

<sup>1</sup> worst peak side lobe ratio

<sup>2</sup> SLCF: different bandwidth

It should be noted that ESA Specifications refer to parameters measured on the transponders. The validation measurements are calculated as the average of the results from both transponders and point targets of opportunity (this explains why the range peak side lobe ratio for UK PAF products is outside the validation threshold).

The measurements always refer to the same area, Flevoland, but not always the same date. The date depends on the products used by the PAF to prepare the validation report. However, it is always October 1991.

These parameters are very stable through time. The standard deviation for these quality indicators for transponder 2 (PRI ESRIN product) in the Flevoland area during the multidisciplinary phase (since April 1992) are:

- range resolution                      0.32 m
- azimuth resolution                    0.47 m
- islrl                                      0.53 dB
- range peak side lobe ratio          0.84 dB
- azimuth peak side lobe ratio        1.3 dB

The radiometric resolution is defined as  $10\log_{10}(1+\sigma/\mu)$ ,  $\sigma$  being the standard deviation and  $\mu$  the mean of the intensity of homogenous distributed targets. Different measurements show that for the different facilities the radiometric resolution is always close to the nominal value:

- 1.98 dB for PRI products
- 3.01 dB for SLC products

### 3.3. SAR Image product troubleshooting

During ERS 1's life time, different problems have appeared in the various image products processed.

These problems are detected by:

- ESA/ESRIN
- PAFs
- External Users via ERS-1 Help Desk

Once a problem is confirmed, there is a discussion with the people concerned in order to clarify exactly the anomaly and the actions to be taken.

Some actions that could be agreed are:



- Modification of the parameters used in the processing
- Reprocessing of the data
- PAF asked for modification
- New version software
- Additional information for the user to correct the problem

The following flowchart shows the methodology used.

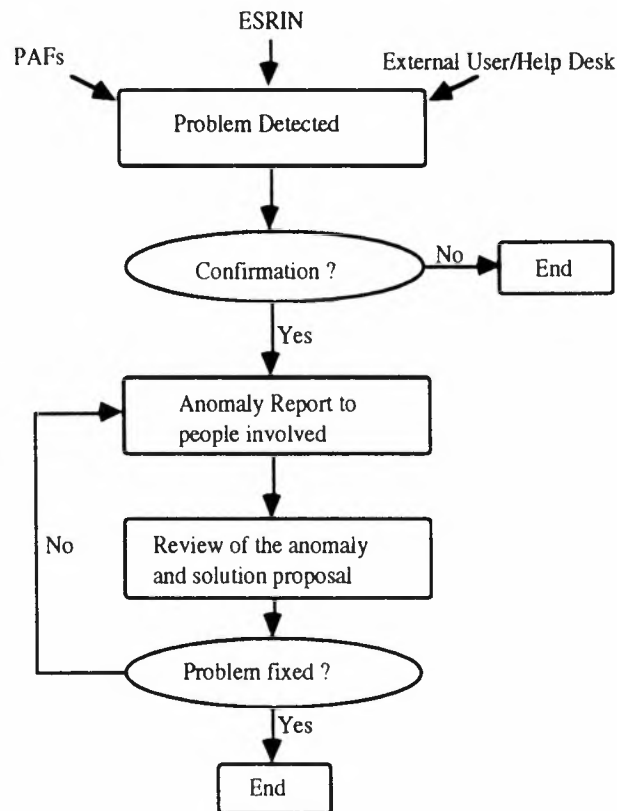


**Figure 6:** Flowchart showing the methodology followed to solve the quality anomalies

Some major problems that have been investigated and fixed during recent months are:

- Antenna Pattern Correction wrongly applied at UK-PAF
- Occasional corruption of the Chirp Data
- CEOS format anomalies
- Incorrect information on the ERS-1 Image catalogue
- Bad data supplied by the PAFs

Let's illustrate these anomalies with some examples:

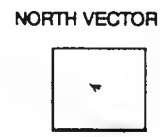
At the beginning of this year, in UK-PAF PRI images over the Greenland area, an anomaly was detected. In near and far range, the images were clearly brighter than in mid range. One of these Greenland images is presented in figure 7. In a normal SAR scene the backscattered power usually decreases from near to far range. After investigations it was found that the antenna pattern correction was applied wrongly. Users affected by this problem were informed and provided with information to solve the anomaly. Some scenes were also reprocessed using the right correction. This anomaly was not detected during the validation checks because the Flevoland and Kent scenes used to verify the correct implementation were not affected by the anomaly. The problem



appeared only at low and high latitudes because the antenna pattern correction wrongly applied was latitude dependent.

PRODUCT ID : 68104 (class 64) VI  
ACQUISITION : 00-JAN-0000 00:00:00.000  
GENERATION : 19-OCT-1992 12:20:02.000  
UK-PAF IMAGE WITH WRONG ANT PAT APPLIED

(78.81 , 321.22) (78.03 , 319.07)  
: corners  
(78.33 , 325.15) (77.58 , 322.83)



ESA/ESRIN

14-SEP-1993 13:11:17


Figure 7: Greenland PRI image with incorrect antenna pattern correction





Another major problem analysed is the corruption of chirp data during telemetry. As the chirp data is used to process the whole scene, the anomaly affects the whole final image. This problem is characterised by strips emerging from bright points. One of these scenes is presented in the figure 8.

After detection and investigation it was decided to improve the chirp quality control before processing and discard the corrupted chirps.

PRODUCT ID : 30858 (class 33) VI	(52.15 , 3.06) (52.35 , 4.43)	NORTH VECTOR
ACQUISITION : 29-JAN-1992 21:47:30.502		: corners
GENERATION : 24-APR-1992 15:44:53.150	(51.27 , 3.40) (51.48 , 4.75)	



ESA/ESRIN

22-JUN-1993 07:18:31

**Figure 8:** Image processed with corrupted chirp data



The third example refers to the geographical information contained in the ERS-1 central catalogue about the different products produced in the PAFs. In early '93 major discrepancies among the nominal co-ordinates (generated before the data acquisition), the information provided by the archiving report and the actual location of the image were found.

Figure 9 shows the frame co-ordinates of one of these scenes. After investigation it was found that the archiving report sent by the PAF was wrong. The PAF fixed the problem and the anomaly was closed.

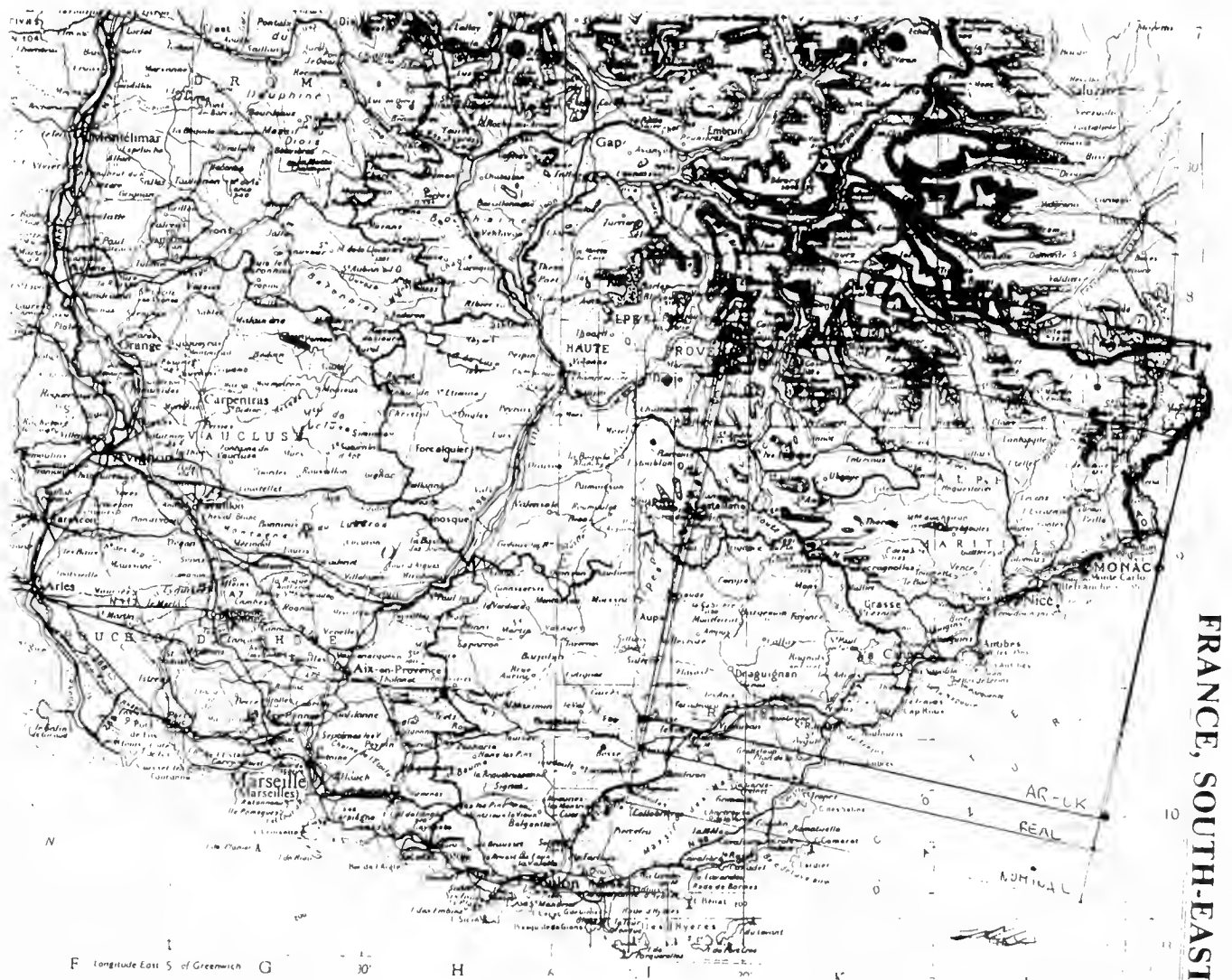


figure 9: Frame location of one PRI product with incorrect archiving report

#### 4. CONCLUSION

This paper has shown the large amount of work that is being invested in the validation and ongoing monitoring of ERS-1 SAR image products. It is important that the products delivered to users have a consistent quality irrespective of ESA processing facility. ESA/ESRINs work in validating ground station and PAF products has been a key issue in guaranteeing this consistency.

We have also illustrated the stability and extremely good performance of the ERS-1 SAR during the first two years of mission.



The experience gained by the ground segment in the analysis and solving of problems and anomalies will be extremely useful for future ESA SAR missions, among them the imminent ERS-2 mission.

#### **ACKNOWLEDGEMENTS**

The authors would like to thank the people involved in the validation of SAR products at the PAFs:

R. Bamler, M. Eineder, A. Roth, B. Schättler (DLR)  
P. Meadows (MRC), R. Cordey, M. Hutchins (DRA)  
L. Candela, E. Lopinto, C. Tarantino (Telespazio)

The authors also acknowledge H. Jackson and Y. L. Desnos (ESA/ESTEC), E. Dwyer and M. Doherty (ESA/ESRIN) for their contribution.

